[Published in *Metrologia* **35**, 761-780 (1998)]

Platinum versus palladium thermocouples: an emf-temperature reference function for the range 0 °C to 1500 °C

George W. Burns and Dean C. Ripple
National Institute of Standards and Technology (NIST), Gaithersburg, MD 20899 (USA)
Mauro Battuello
CNR Istituto di Metrologia "G. Colonnetti" (IMGC), Torino (Italy)

Abstract

We present an emf-temperature reference function for platinum versus palladium (Pt/Pd) thermocouples in air for the range 0 °C to 1500 °C. The reference function is based on the International Temperature Scale of 1990 (ITS-90) and has an expanded uncertainty (coverage factor of two) of less than the equivalent of 11 mK for temperatures up to 1050 °C and rising smoothly to approximately 0.3 K at 1500 °C. The reference function is based on a set of Pt/Pd thermocouples of exceptional stability and homogeneity constructed from Pt and Pd wire of very high purity (99.999% mass fraction and 99.997% mass fraction, respectively). Experimental results are presented on the thermoelectric stability of Pt/Pd thermocouples at high temperatures and on the calibration of Pt/Pd thermocouples based on this reference function.

1. Introduction:

Thermocouples constructed from Pt-Rh alloys and pure Pt are currently the predominant choice for use as a secondary reference standard [1]. Type S (Pt-10%Rh vs. Pt) and type R (Pt-13%Rh vs. Pt) thermocouples are used throughout the temperature range from 0 °C to approximately 1400 °C, and type B (Pt-30%Rh vs. Pt-6%Rh) thermocouples generally are used over the range from 800 °C to 1700 °C. The smallest expanded uncertainty [2] (coverage factor *k*=2) obtainable with any of the Pt-Rh alloy thermocouples is 0.1 K at 1000 °C [3,4,5] as a consequence of preferential oxidation of Rh [6,7,8]. In contrast, thermocouples constructed from pure elements do not suffer from such preferential oxidation problems [9,10]. This fact has two important consequences: pure element thermocouples are inherently more thermoelectrically homogeneous, and their thermoelectric stability is not limited by changes in alloy composition caused by preferential oxidation. The thermoelectric stability and homogeneity of Au versus Pt (Au/Pt) thermocouples have been reported previously [9,10], but the low melting point of Au (1064.18 °C) and the incompatibility of Au with some semiconductor processes limit the use of these thermocouples. Previous reports on the properties of Pt/Pd thermocouples demonstrated that the stability and homogeneity of Pt/Pd thermocouples indeed can be far superior to that of the best Pt-Rh alloy thermocouples and that they could readily be used at temperatures much higher than that of the Au freezing point [11,12,13,14]. Oxidation of the Pd thermoelement in the range 500 °C to 800 °C causes small thermoelectric shifts in Pt/Pd thermocouples, but these effects are reversible with proper annealing techniques [13].

A proposal from IMGC [11] led to a joint study between NIST and IMGC to determine an emf-temperature reference function for Pt/Pd thermocouples used in air. The two laboratories agreed to perform measurements on a set of thermocouples prepared from the highest-purity Pt and Pd available and to cover a broad range of temperatures. For this study, NIST developed the procedure for annealing the thermocouples, prepared the thermocouples that were used in the study, and evaluated the thermocouples for thermoelectric stability and homogeneity. Also, fixed-point data were obtained at NIST for all of the thermocouples. Then, a set of three thermocouples was delivered to IMGC. IMGC obtained further fixed-point data and then made measurements by comparison with a radiation thermometer in the range 800 °C to 1500 °C. At NIST, four Pt/Pd thermocouples were calibrated by comparison methods, using as reference thermometers a standard platinum resistance thermometer (SPRT) up to 450 °C and a set of Au/Pt thermocouples from 419 °C to 1000 °C. Following the comparison testing at IMGC and NIST, the four thermocouples calibrated by comparison methods at NIST and one of the thermocouples calibrated at IMGC were again calibrated in fixed-point cells at NIST. A statistical analysis of all of the data was performed at NIST, and a reference function was generated from a selected subset of data. IMGC performed additional comparison measurements between Pt/Pd thermocouples and a radiation thermometer to measure the stability of the thermocouples at high temperature, and NIST performed additional comparison measurements between a variety of thermocouples as a check on the validity and utility of the reference function.

Several published papers have reported reference functions for Pt/Pd thermocouples [12,15,16]. The work reported in this paper differs from prior work in that the purity of the Pd used was significantly higher, the highest temperature of the measurements was 1500 °C, and the uncertainty of the data is significantly smaller.

This paper is organized as follows. Section 2 describes the preparation of the thermocouples, Section 3 discusses the experimental procedures and apparatus, and Section 4 summarizes the data. Section 5 describes the components of uncertainty of the data. The selection of data for the reference function is described in Section 6; Section 7 explains how the reference function was obtained from the data; and Section 8 gives the uncertainty of the reference function. Section 9 presents the results of calibrations of several Pt/Pd thermocouples constructed with Pd wire from various lots and of various purities. Section 10 gives the results of some drift tests at high temperatures, and Section 11 compares the results of the present work with data and reference functions from the literature.

2. Preparation of thermocouples

The Pt/Pd thermocouples used to determine the emf-temperature reference function were constructed at NIST using a single lot of 0.5 mm diameter Pd wire of 99.997+% purity and 0.5 mm diameter Pt wire of 99.999% purity. These Pd and Pt wires were manufactured by Johnson Matthey (UK) and Sigmund Cohn Corporation (USA), respectively.* A spectrochemical analysis of the Pd wire is given in Table 1. The high purity of the Pt wire was attested to by its close thermoelectrical agreement with the NIST-maintained Pt thermoelectric standard, Standard Reference Material SRM-1967, commonly referred to as Pt-67 [17]. The emf of the Pt wire versus Pt-67 at 1064 °C, with the reference junction at 0 °C, was found to be +1.4 μV.

Prior to constructing the thermocouples, the Pt and Pd wires were annealed in air. Extensive preliminary measurements had been performed at NIST with six lots of 0.5 mm diameter Pd wire to identify the wire lot and annealing method for the Pd thermoelement that would produce the most stable thermocouple emf. The Pd-wire lots studied included two lots of the 99.997+% purity wire manufactured by Johnson Matthey (UK) and four lots of 99.95% to 99.98% purity wire obtained from three manufacturers in the USA. The Pd wires from the lot selected were annealed electrically for 10 h at 1300 °C, then in a furnace for 1 h at 1100 °C, and finally in a furnace overnight at 450 °C. The Pt wires were annealed following a procedure similar to that used for Au/Pt thermocouples [9,10]. All of the Pt wires were annealed first electrically for 10 h at 1300 °C and then 1 h at 450 °C, then annealed in a furnace for 1 h at 1100 °C, and finally overnight at 450 °C. For the furnace anneals, segments of the wire were pulled into the bores of a four-bore alumina tube (1.2 mm diameter bores, 4.7 mm outer diameter, 76 cm long) of 99.8% purity. A separate alumina tube was used with each metal. The tube holding the wires was placed into an alumina protection tube mounted in the furnace described in Section 3.1. The wire segments (≤63 cm) were short enough that during a furnace anneal they were located in a zone of the furnace that was uniform in temperature to within ±2 K.

Construction of the Pt/Pd thermocouples closely followed the practice recommended [9] for Au/Pt thermocouples. The thermocouples were mounted in twin-bore alumina tubes of 99.8% purity that had been baked in air for 50 h at 1200 °C before being used. The tubes were 76 cm long, 4.7 mm in diameter and had 1.6 mm diameter bores. During the assembly of the thermocouples, either a Pt or Pd pull wire was used to thread the annealed wires gently into the bores of the tubes, and the wire segments were rejoined by butt-welding with a small hydrogen-oxygen torch. Each thermocouple was 1.6 m long. The thermocouple wires emerging from the alumina tube were insulated with flexible fiber-glass tubing to within 2 cm of their ends, and the fiber-glass tubing was joined to the alumina tube with heat-shrinkable sleeving. A bar-type clamp was installed that compressed the fiber-glass tubing against the thermoelements to anchor them near the end of the alumina tube. The Pt and Pd thermoelements were connected at the measuring junction by an expansion coil constructed from 0.12 mm diameter Pt wire that was wound into a coil of four turns of 1 mm diameter. A pair of insulated Cu wires was soldered to the other ends of the thermoelements to form the reference junctions.

After construction, each thermocouple was furnace annealed in air for 50 h at 1100 °C, and we determined the effects of inhomogeneity of the thermocouple by measuring its emf on insertion into and withdrawal from a Ag freezing-point cell during a freeze of the Ag. For this measurement, the test thermocouple was inserted into the cell, after a freeze was induced, to a point where the measuring junction was held 2 cm above the surface of the Ag. After 25 min at this position, the thermocouple was inserted in steps of 2 cm every 5 min. The thermocouple was held at full immersion (18 cm below the surface of the Ag) for 25 min, and then withdrawn in steps of 2 cm every 5 min, after an initial step of 1 cm. At immersions greater than 6 cm, the thermocouple measuring junction was in thermal equilibrium with the freezing metal. The dependence of the emf value on the hydrostatic head is less than the equivalent of 1 mK for immersions ranging from 6 cm to 18 cm. Thus, any deviation from a constant value of emf was taken as an indication of inhomogeneity or drift of the thermocouple. The spread in emf values for all measurements at immersions of 6 cm and greater was calculated and defined as the inhomogeneity. If the inhomogeneity exceeded the equivalent of 20 mK, the Pd wire of the thermocouple was replaced, the thermocouple was reassembled and annealed for 50 h at 1100 °C, and its immersion profile in the Ag freezing-point cell was remeasured.

After obtaining a set of seven thermocouples that met the homogeneity requirement, each of the thermocouples was furnace annealed for an additional 450 h at 1100 °C to verify its thermoelectric stability. Figure 1 shows the designations of the seven thermocouples and the results of heat treatment on the thermocouples. The furnace anneal at 1100 °C for 500 h reduced the drift in the thermocouple emf at the Ag freezing point to the equivalent of less than 10 mK/100 h at 1100 °C. Measurements of thermocouples constructed from the same wire lots as these seven thermocouples and heated for as long as 1900 h at 1100 °C during preliminary studies indicated that the drift in the thermocouple emf is caused not by impurities transferred to the thermoelements from the alumina tubes, or by thermoelectric changes in the Pt wires, but by some other cause intrinsic to the Pd wire [13]. Furthermore, after 1200 h of heating at 1100 °C, no further drift in the thermocouple emf was detected.

3. Experimental procedures and apparatus

3.1 Measurements at NIST

All of the emf measurements were made with a calibrated digital multimeter (Hewlett-Packard model 3458A) and scanner (Hewlett-Packard model 3495A) system. All resistance measurements of the SPRT were made with a model F18 ac resistance-ratio bridge manufactured by Automatic Systems Laboratories, Inc. The thermocouple and SPRT data were obtained automatically via a computer-controlled IEEE-488 bus and logged to a data file for later analysis. The reference junctions of the thermocouples were maintained at 0 °C in an ice bath when measurements were made. The reference junctions were contained in closed-end glass tubes (6 mm outer diameter, 4 mm inner diameter) and were immersed 22 cm in the ice bath, which was contained in a cylindrical Dewar flask (7 cm inner diameter and 30 cm deep) having a polyethylene-foam cover.

A 1.1 m long horizontal-tube furnace with a closed-end alumina protection tube (22 mm inner diameter) was used to anneal the assembled thermocouples as well as the Pt and Pd wires prior to constructing the thermocouples. During a heat treatment, the temperature along the portion of the thermocouple extending from its measuring junction to approximately 62 cm from the junction was uniform within ±2 K. A length of less than 55 cm of the thermocouple was heated above room temperature when the thermocouple was tested in the various other equipment used in this work.

Freezing-point cells containing Au, Ag, Al, Zn, Sn, and In were used in the evaluation and measurement of the thermocouples. The well of each freezing-point cell contained a silica glass protection tube (8 mm outer diameter, 6 mm inner diameter) closed at one end, open to air at the other end, and matte finished on the outer surface to minimize heat losses by radiation piping. At full immersion of the thermocouple into the freezing-point cells, the measuring junction of the thermocouple was 18 cm below the surface of the metal. Freezes in the Au, Ag, and Al cells were performed in a vertical furnace containing a 61 cm long sodium heat pipe. Freezes in the Zn, Sn, and In cells were performed in a single zone furnace having an Al moderating block. For all of the freezing points, the furnace was held 0.5 °C below the freezing-point temperature after the freeze was initiated, and the freeze was induced internally by inserting an alumina insulator, initially at room temperature, into the cell.

Measurements of the thermocouples at the ice point used a properly prepared ice bath [18] contained in a cylindrical Dewar flask (7 cm inner diameter and 41 cm deep). The test thermocouple was contained in a closed-end glass tube (7 mm outer diameter, 5 mm inner diameter) inserted in the tightly packed mixture of ice and water in the flask. Its measuring junction was located 35 cm below the surface of the ice-water mixture when measurements were made.

Measurements to determine the emf versus temperature relation of the Pt/Pd thermocouples used stirred liquid baths in the temperature range 15 °C to 450 °C. In the stirred liquid baths, the temperature of the bath was determined with a 25.5 Ω SPRT (Chino model R800-2) calibrated on the ITS-90 [19]. A water bath was used from 15 °C to 95 °C, an oil bath from 95 °C to 275 °C, and a salt bath from 275 °C to 450 °C. During measurements in each bath, each thermocouple was contained in a borosilicate glass tube (7 mm outer diameter, 5 mm inner diameter) that was closed at the bottom. Each thermocouple was positioned such that its measuring junction was at the same immersion (35 cm below the liquid surface) in the bath as the midpoint of the sensing element of the SPRT. In each bath, the temperature of the sensing element of the SPRT and that of the measuring junction of each test thermocouple differed by not more than 5 mK, based on previous measurements of the temperature uniformity of each bath using three SPRTs.

For the temperature range 419 °C to 1000 °C, the Pt/Pd thermocouples were calibrated by comparison with a set of three Au/Pt reference thermocouples (designated Au/Pt 91-10, Au/Pt 93-1, and Au/Pt 94-2) using a comparator cell heated in the same furnace that was used with the Au, Ag, and Al freezing-point cells. The reference thermocouples had been constructed by the procedures described previously [10] using three separate lots of 0.5 mm diameter Au and Pt wires of 99.999% purity that were purchased in 1991, 1993, and 1994 from the Sigmund Cohn Corporation (USA). Each reference thermocouple had been calibrated at the freezing points of Ag, Al, Zn, Sn, and In and at the ice point. The comparison cell was comprised of a cylindrical Cu block, 25 cm long by 4.5 cm in diameter, contained in an outer silica-glass tube and held in an atmosphere of Ar at 101 kPa pressure. For each run in the comparison cell, two Pt/Pd thermocouples and one Au/Pt reference thermocouple were inserted into an inner silica-glass tube, 1.1 cm in inner diameter, that was located on the axis of a single bore of the Cu block. A stainless steel flange at the top of the cell was sealed to both the outer silica-glass tube and the inner tube, so that the Cu block could be surrounded by Ar gas and the thermocouples in the inner tube were exposed to air. Along the bottom 12 cm of the block, the temperature was uniform to ±10 mK, as determined during preliminary measurements with two Au/Pt thermocouples. To make accurate measurements in the comparator cell, the thermocouples were modified so that the measuring junctions of all three thermocouples were maintained at the same temperature. This was accomplished by forming a measuring junction common to all three thermocouples in the following manner. First, the Pt expansion coils were removed from all three thermocouples. Second, each thermoelement was extended by welding to it a 1.5 cm length of high purity, 0.12 mm diameter Au, Pt, or Pd wire. Finally, these fine wires were welded into a common measuring junction, leaving sufficient slack in the wires to minimize the effects of the different thermal expansions of the three metals.

The emf measurements proceeded in four steps. First, the emf of each of the seven Pt/Pd thermocouples was measured at the freezing points of Au, Ag, Al, Zn, Sn, and In and at the ice point. These measurements were taken in descending order in temperature, Au to ice. The immersion profile of each thermocouple was also measured in Au, Ag, and Al freezing-point cells. Then three of the thermocouples (designated JM93-12, JM93-13, and JM93-16) were sent to IMGC for measurements over the range 800 °C to 1300 °C. Second, comparison calibrations of the other four thermocouples (designated JM93-2, JM93-11, JM93-14, and JM93-15) with the SPRT were made in stirred liquid baths, beginning at 15 °C and increasing to 450 °C. The comparisons were taken at approximately 15 °C intervals from 15 °C to 75 °C, at approximately 20 °C intervals from 75 °C to 275 °C, and at approximately 25 °C intervals at temperatures above 275 °C. Third, comparison calibrations of the thermocouples with Au/Pt reference thermocouples were made in the Cu comparator cell at 20 °C to 40 °C intervals, beginning at 419 °C and increasing to about 1000 °C. Each of the four Pt/Pd thermocouples was tested against each of the three Au/Pt thermocouples. The measurements during each of the six comparator runs that were conducted required approximately 30 h to complete. Finally, the emf of each Pt/Pd and Au/Pt thermocouple was measured at each fixed point to confirm the stability of the thermocouple during the measurement process. These fixed-point measurements, like those performed prior to the comparison runs, were taken in descending order in temperature, Au (Ag for the Au/Pt thermocouples) to ice, and included determinations of the thermocouple immersion profiles in the Au, Ag, and Al freezing-point cells. During all four steps, whenever a thermocouple was heated to a temperature above 450 °C and then cooled to room temperature, it was given a maintenance anneal before the next measurement, using a previously determined annealing procedure [13]. For the Pt/Pd thermocouples, the maintenance anneal in air consisted of a furnace anneal for 30 min at 1070 °C, a quench to room temperature, and an 18 h furnace anneal at 450 °C. For the Au/Pt thermocouples, the procedure was a 1 h furnace anneal at 975 °C, a slow cool in the furnace over about 3.5 h to 450 °C, followed by an overnight anneal at 450 °C.

3.2 Measurements at IMGC

After the Pt/Pd thermocouples JM93-12, JM93-13 and JM93-16 were received from NIST, they first were measured at the Al and Ag fixed points using the freezing-point cells [20] normally used for calibrating HTPRTs on the ITS-90. All subsequent measurements of the thermocouples at fixed points were made using a version of the fixed-point blackbodies [21] used for radiation thermometry, arranged in a geometry suitable for the thermocouple measurements. Following the initial check at fixed points, each thermocouple was calibrated by comparison with the IMGC primary standard radiation thermometer [22]. The measuring junction of the thermocouple was located adjacent to a specially designed blackbody cavity heated within a horizontal tube furnace. Measurements of the emf of each thermocouple and of the cavity temperature with the radiation thermometer were made at approximately 50 °C steps from 800 °C to 1300 °C. At each measuring point the thermocouples were inserted successively into the furnace. Following these measurements, each thermocouple was measured again at the Ag fixed point and then retested against the radiation thermometer in a second comparison run from 800 °C to 1300 °C. During the two comparison runs each thermocouple was heated for a total of about 60 h, with the exposure time at the different temperatures being approximately the same. After the second run, the emf of each thermocouple was measured again at the Ag fixed point and then measured at the Cu fixed point. Thermocouple JM93-12 then was returned to NIST, where it was measured at the Au, Ag, Al, Zn, Sn, In, and ice fixed points. No discernible changes were detected in the inhomogeneity of JM93-12. Furthermore, its emf values at the fixed points agreed with those measured prior to delivery to IMGC to within the equivalent of 11 mK. Thermocouple JM93-12 was returned to IMGC, along with thermocouple JM93-11, and they were tested by comparison with the radiation thermometer at approximately 50 °C steps from 1350 °C to 1500 °C. Both thermocouples then were measured at the Ag fixed point.

The signals of the thermocouples and radiation thermometer were measured with a Hewlett-Packard model 3458A digital multimeter. The reference junctions of the Pt/Pd thermocouples were maintained at 0 °C in an ice bath when measurements were made.

A sectional view of the blackbody assembly used as a transfer source for the comparison measurements between the thermocouples and the radiation thermometer is shown in Figure 2. The blackbody assembly was heated in a furnace having molybdenum disilicide heaters and a horizontal alumina tube (65 mm inner diameter). The cylindrical blackbody cavity, 6 mm in diameter and 67 mm long, was constructed from cylindrical blocks that were produced by bonding Al_2O_3 and SiC powders. This composite material was found [14] to have a normal spectral emissivity at 900 nm of greater than 0.9, as measured with an integrating sphere reflectometer. Based on such a value for the wall emissivity, the effective emissivity values of the cavity calculated for actual operating conditions ranged from 0.99964 to 0.99968. A type S differential thermocouple with its measuring and reference junctions 10 mm apart was inserted in the lateral well in the blocks to measure the temperature uniformity. Additional heaters made from 0.5 mm diameter Pt wires and mounted in alumina tubes were positioned on both sides of the cavity. These heaters were movable and their positions were adjusted to obtain a nearly uniform temperature for a distance of about 70 mm, as measured from a point 20 mm in front of the back wall of the blackbody cavity to a point approximately 50 mm from the end of the well containing the Pt/Pd thermocouple.

The standard radiation thermometer [22] used in this work was a fixed focus instrument having a working distance of 460 mm and a minimum required target size of 1.1 mm. It can be operated at a band centered at either 655 nm or 900 nm, as determined by two interchangeable interference filters having half-peak bandwidths of 12.7 nm and 14 nm, respectively. The instrument uses a photomultiplier or a silicon photodiode as a detector, depending on whether the band at 655 nm or that at 900 nm is selected. In this work, the band at 900 nm was used for all measurements, and the detector was a Hamamatsu model S1336-44BQ silicon photodiode operated in an unbiased mode and with its temperature controlled at 28 °C.

The radiation thermometer, which had been previously characterized for its spectral responsivity and non-linearity, was used as a flux comparator in this experiment. It compared the radiance of the blackbody cavity to that of a tungsten-strip lamp of the High-Stability type from the General Electric Co., UK, maintained at the radiance temperature of the Ag point. The temperature of the cavity was obtained from the measured radiance ratio by applying the defining equation [19] of the ITS-90.

4. Experimental Results

In the first round of testing in fixed-point cells, the seven thermocouples prepared for determination of the reference function demonstrated excellent homogeneity and a relatively narrow spread in emf values at each fixed point. For example, the distribution of emf values at the Ag point had a standard deviation of 0.30 μV, equivalent to 15 mK. An immersion plot for thermocouple JM93-15 at the Ag point is shown in Figure 3. The total spread in emf values over a 12 cm range of immersions is 0.07 μV at the Ag point, or 0.03 μV when expressed as a standard deviation of the measured emf from the emf at full immersion. At the Al point, the inhomogeneity of JM93-15 is 0.03 μV when expressed as a standard deviation, over a 12 cm range of immersions.

The round of fixed-point testing on JM93-2, JM93-11, JM93-14, and JM93-15 that followed all of the tests in the stirred liquid baths and in the Cu comparator block gave inhomogeneity values that were very similar to the values measured initially. The emf values in the second round of testing were slightly lower, by an average of 0.07 μV at the Ag point, equivalent to 4 mK. This difference is quite small considering that each thermocouple was exposed to temperatures above 420 °C for approximately 100 h between the two rounds of fixed-point testing. The Au/Pt thermocouples used as reference standards also were tested twice in fixed-point cells, both before and after the comparison runs. The difference in emf values for all three Au/Pt thermocouples for the two rounds was less than the equivalent of 3 mK at all fixed points, and there was no evidence of instability in the emf values or an increase in inhomogeneity for any of the thermocouples.

The measurements at NIST and IMGC were conducted in a number of different apparatuses. The data in every apparatus overlapped data taken in another apparatus for at least some range of temperature values. All of the fixed-point data overlapped data taken in stirred liquid baths or the comparator block; the data taken in different baths overlapped; fixed point measurements were performed at IMGC as well as NIST; and the radiometric data overlapped both fixed-point data and data from the comparator block. Figures 4 and 5 show the deviations from the NIST/IMGC reference function of the data used for the determination of the reference function. The selection of data and the determination of the reference function are discussed in Sections 6 and 7, respectively. With only one exception, the data in the regions of overlap agreed within the expected experimental uncertainties.

The measurement taken in the oil bath at 95 °C during run 1 disagreed with the corresponding point obtained in the water bath. Multiple repeat measurements in the oil bath during run 2 did agree with the water bath data and demonstrated that this one point was an outlier. Because we could find no internal inconsistency with the run 1 point, it was not discarded from the data set.

The measurements in the Cu comparator block at temperatures near 962 °C gave emf values that were lower than the values obtained in the Ag freezing-point cell. This effect was comparable to the drop in emf of Pt/Pd thermocouples caused by oxidation of the Pd thermoelement found in previous work [13]. The oxidation effect is discussed quantitatively in the next section.

The results of the radiometric measurements at IMGC showed no significant differences between the measured emf values of JM93-11, JM93-12, JM93-13, and JM93-16. This result was anticipated, since the spread in emf values at the fixed points was small relative to the repeatability of the radiometric measurements. After data were obtained over the range 800 °C to 1300 °C, thermocouple JM93-12 was returned to NIST for remeasurement in fixed-point cells, as described in Section 3.2. The emf of this thermocouple was lower than the initial fixed-point values by 0.22 μV at Au and 0.11 μV at Ag. This change is insignificant compared to the precision of the radiometry. After measurement at the fixed points, JM93-12 was returned to IMGC for additional measurements from 1350 °C to 1500 °C.

5. Summary of uncertainties

The uncertainties of the data are summarized in Table 2 and are discussed below. Within the set of data points that include a particular subcomponent u_i of the standard uncertainty, the magnitude of u_i varies for each datum point. Table 2 lists the minimum and maximum values of this range of u_i values.

5.1 Uncertainties of measurements at NIST

Repeated measurements in fixed-point cells on the four Pt/Pd thermocouples JM93-2, JM93-11, JM93-14, and JM93-15 were used to determine the Type A uncertainty of the measurements at NIST. When expressed as an equivalent temperature uncertainty, there was no statistical difference between the uncertainties at the different fixed points. A pooled value of the standard uncertainty for all of the fixed point measurements is 3.4 mK, with 28 degrees of freedom. In Table 2, this uncertainty is termed the "Repeatability of Pt/Pd TCs", but more accurately can be considered to include also effects of the repeatability of the emf measurements, the repeatability of the reference junction bath, the thermoelectric instability of the thermocouples over the course of the comparison measurements, and the repeatability of the fixed-point realizations.

Uncertainties of the emf measurements not covered in the Type A uncertainty were determined by independent measurements of the variation of the thermal emfs from the scanner relays and wiring, calibration of the digital multimeter by the Electricity Division of NIST, measurements of the gain stability of the multimeter over extended periods of time, and by intercomparison of the multimeter with other multimeters of the same and different manufacturer. The Type B standard uncertainty for the combined scanner and digital

multimeter system can be expressed as $u/\mu\text{V} = 2.3\times10^{-6}(E/\mu\text{V}) + 0.01$, where E is the thermocouple emf.

For data obtained in the stirred liquid baths, there are Type B uncertainties to account for gradients in the bath and for the calibration and measurement accuracy of the SPRT used to determine the temperature.

For measurements at each fixed point, a Type B uncertainty was included to account for deviations of our cells from an ideal fixed point of a pure material. These deviations were determined by measurements of freezing plateaus with an SPRT or a high temperature SPRT, by intercomparison with the reference standard cells maintained by the Platinum Resistance Thermometry Laboratory at NIST, and by estimation of uncertainty from known impurities. The fixed-point temperatures listed in Table 10 include a correction for the hydrostatic head and a correction for the temperature difference between the cells used for this study and the reference standard cells maintained in the Platinum Resistance Thermometry Laboratory.

Measurements in the range from 419 °C to 1000 °C utilized Au/Pt thermocouples as reference thermometers. The uncertainty of the calibration of these thermometers was determined from a separate analysis of Au/Pt thermocouples that includes the terms outlined above and an additional term for the uncertainty of modeling deviations of the emf of the Au/Pt thermocouple from the reference function [10] with a quadratic function. The resulting standard uncertainty for the Au/Pt thermocouples ranged from 2.7 mK at 419 °C to 4.5 mK at 962 °C to 7.5 mK at 1000 °C.

The method of joining the Pt/Pd and Au/Pt thermocouples in the well of the comparator block, together with the low thermal gradients inside the well, ensured that differences between the temperatures of the measuring junctions of all the thermocouples in each comparison run were negligible.

There was a systematic effect in the comparator block data that dominates the uncertainty for temperatures in the range 850 °C to 1000 °C. At temperatures above 500 °C, oxidation causes a measurable shift of the thermoelectric properties of Pd. *In situ* tests of the stability of the emf of a Pt/Pd thermocouple at a fixed immersion have shown a reduction in emf of 0.28 μV after 60 h of aging at the Ag freezing point, 961.78 °C [13]. This effect is cumulative, but may be reversed by exposing the oxidized wire to temperatures sufficiently high to decompose the oxide, such as occurs during the maintenance anneal procedure. Each comparison run lasted approximately 30 h, and during this time the emf of the Pt/Pd thermocouples dropped continuously below the emf values of a thermocouple in the just-annealed state. Because the comparison runs began at 419 °C and proceeded to higher temperatures, the oxidation effects are most pronounced at the higher temperatures. As seen in Figure 4, the discrepancy at the Al freezing-point temperature between the fixed-point and comparison data is approximately 0.08 μV, but at the Ag freezing-point temperature, the discrepancy has increased to approximately 0.17 μV.

The oxidation effect cannot be modeled accurately enough to correct the comparison data, but the uncertainty of the comparison data from this effect can be quantified. A 5th order polynomial was fitted to one data set that included all of the comparator block data and fixed-point data up to the Zn freezing point. The same polynomial form was then fitted to another data set that included the comparator block data up to 600 °C and all of the fixed-point data. For both fits, the rms deviations from the fits were approximately 0.05 μV. The difference between the two fits is a measure of the shift of thermocouple emf from oxidation effects over the full temperature range of the comparator block data. A simple linear approximation to the absolute value of the difference was used as the component of the standard uncertainty of the comparator block data corresponding to the oxidation effect: $u_{ox}/\mu V = 0.0011(t_{90}/°C - 800)$, for $t_{90} \geq 800$ °C.

The contribution of inhomogeneity of the Pt/Pd thermocouples to the uncertainty of the emf values can be estimated from the thermal profiles of the different baths and furnaces used and from the measured immersion profiles in the Al and Ag fixed-point cells. The comparison measurements against Au/Pt thermocouples and the measurements in the Al, Ag, and Au fixed-point cells were all performed in a single furnace where the distance from the measuring junction to the point of maximum thermal gradient was 44 cm. For these points, no extra uncertainty was assigned. Measurements in the stirred liquid baths have an immersion of approximately 9 cm less, and measurements in the In, Sn, and Zn fixed-point cells have an immersion of 6 cm less. For the points with immersions different from 44 cm by the length *l*, the standard uncertainty for thermocouple inhomogeneity, u_{inh}, was assumed to vary linearly with temperature, equaling zero at 0 °C and rising to a value at 660 °C of

$$u_{inh}(660\,°C) = \left| E_{Al}(44\,cm) - E_{Al}(44\,cm - l) \right|.$$

As seen in Table 2, no single uncertainty component dominates the combined uncertainty. For the fixed-point measurements, thermocouple repeatability and the uncertainty of the emf measurements are the dominant uncertainties. In the stirred bath measurements, bath gradients, uncertainty of the emf measurements, and repeatability of the thermocouples are comparable in magnitude. The uncertainty of measurements in the comparator block is dominated by the subcomponent for the oxidation effect for temperatures above about 900 °C, but for lower temperatures, the calibration of the Au/Pt thermocouples, the repeatability of the Au/Pt and Pt/Pd thermocouples, and the uncertainty of the emf measurements are all significant.

5.2 Uncertainties of measurements at IMGC

For the radiometric measurements in the range 800 °C to 1300 °C, two separate runs of data with three separate thermocouples were obtained. A Type A uncertainty of the repeatability of the measurements was derived by normalizing all of the data at each temperature and then calculating the standard deviation of the emf values at each temperature. There was no significant temperature dependence of this standard deviation, so the standard deviation values were pooled to give a single Type A standard uncertainty of 50 mK. For the range 1350 °C to 1500 °C, the data were obtained in only one run with only two thermocouples. This amount of data was insufficient to obtain a reliable value for the repeatability, so conservative estimates obtained from previous experiments were used to assign a Type B uncertainty for the repeatability. The uncertainty for the repeatability of the measurements is the largest component in the combined uncertainty, especially at temperatures of 1350 °C and above.

The effects of thermocouple inhomogeneity are implicitly included to some extent in the Type A uncertainty for the repeatability because this uncertainty was calculated from the spread of measurements of multiple thermocouples. Because the inhomogeneity of the tested thermocouples is a small effect compared to other limitations on the accuracy of the IMGC radiometric measurements, no further uncertainty for this effect has been included.

The uncertainty component associated with the “Radiation thermometer calibration” has been estimated on the basis of the present uncertainty assigned to the ITS-90 realization at IMGC and on an allowance for possible variations in the spectral responsivity of the thermometer, which was measured a few months before this experiment. This uncertainty is a significant component to the combined uncertainty for temperatures of 1300 °C and below.

The different geometry of the furnaces used for the fixed-point calibration of the radiation thermometer and for measurements with the Pt/Pd thermocouples required a correction to be made on the experimental data to account for contributions due to the size-of-source effect (SSE). The geometrical distribution of the SSE, measured with an integrating-sphere apparatus, was used to correct the data. Table 2 lists the residual Type B uncertainty after the correction has been applied. The emissivity of the blackbody cavity was calculated based on the measured emissivity of the Al_2O_3/SiC material used for the blackbody and on the measured temperature profile along the cavity. The cavity emissivity exceeded 0.9996 at all temperatures, and the data were corrected using the calculated value of emissivity at each temperature. Table 2 lists the residual, Type B uncertainty after this correction has been applied.

A Type B uncertainty was included for the uncertainty of the instruments used to measure voltage. This component is essentially the uncertainty of the measurement of the thermocouple emf with the digital voltmeter.

6. Selection of data used for determination of the reference function

The use of a least-squares fitting procedure to determine the parameters of an emf-temperature relationship of a thermocouple type is valid only if all of the data included in the fit are from one thermocouple or if the data are from a set of thermocouples that are not statistically distinguishable in their thermoelectric properties. This section describes the selection of a subset of data that meets the above criteria.

The thermocouples delivered to IMGC were tested at NIST at a full set of fixed points prior to any radiometric measurements. The maximum spread of the measured thermocouple emf values at the Ag freezing point was 0.5 μV. This is substantially smaller than the 2.7 μV expanded uncertainty of the radiometric measurements at this temperature, and the thermocouples could not be statistically distinguished on the basis of the radiometric measurements. Therefore, at temperatures above 962 °C, data from all of the thermocouples were used to obtain the reference function. There were small but statistically significant differences between the results of the first and second radiometric comparison runs: the emf of the second run was higher than that of the first run by an average of 0.7 μV over the range 800 °C to 1300 °C [14]. For this reason, and because the thermocouples were not given a maintenance anneal prior to the second run, we used only the results from the first radiometry run for the temperature range 800 °C to 1300 °C. For the range 1350 °C to 1500 °C, there was only one run, and all of the data were used. Both thermocouples in this run, JM93-11 and JM93-12, were given maintenance anneals prior to the run.

Below 1064 °C, the precision of the data is very high, and the data from the different thermocouples tested at NIST are statistically different. We chose one thermocouple, JM93-15, that had the following desirable properties:

1. The emf values measured at the fixed points before and after the comparison runs agreed to within 0.05 μV.
2. The emf values at the fixed points for JM93-15 were very close to the average of the values for the thermocouples used in the measurements at IMGC.
3. The homogeneity of JM93-15 was among the best of all thermocouples tested.
4. The comparison data agreed very well with the fixed-point data.

One of the thermocouples tested at IMGC, JM93-16, had emf values at the fixed points that agreed with those of JM93-15 to within the mutual uncertainty of the fixed-point values for the two thermocouples. The fixed-point emf values and the IMGC radiometric data from 800 °C to 1000 °C for JM93-16 were also included in the data set used for the determination of the reference function.

The complete set of data is shown at the end of the paper (see Table 10). A total of 142 data points were used.

7. Determination of the form of the reference function

The full set of data covering the range 0 °C to 1500 °C was modeled by several trial functions, with parameters for each function determined by the method of least squares. Over this range, the uncertainty of the data varies by a factor of approximately 100. Therefore, each datum used in the least squares fit was appropriately weighted by its combined standard uncertainty. Because the difference between the IMGC and the NIST data in the region of overlap, 800 °C to 1064 °C, was not significant compared to the combined measurement uncertainty, no attempt was made to offset the emf values of one set of data to match the other set.

Both spline polynomials and simple polynomials were considered as possible forms of the reference function. The spline functions had continuous values of the emf and of the first and second derivatives of emf with respect to temperature at the internal breakpoints. No constraint was placed on the second derivative at the upper and lower temperature boundaries of 1500 °C and 0 °C, respectively. The software used for the least squares fitting allowed adjustment of the polynomial order of each subrange of the spline functions, independent of the other subranges. For improved numerical accuracy, the temperature was expressed as $t_R = (t_{90} - t_{LO,k}) / (t_{HI,k} - t_{LO,k})$, which varies between values of 0 and 1 between the temperature at the lower boundary point or breakpoint of subrange k, $t_{LO,k}$, and the temperature at the upper boundary point of the subrange, $t_{HI,k}$. The

$$E = a_0 + \sum_{i=1}^{N_k} a_i \left[(t_{90} - t_{LO,k}) / (t_{HI,k} - t_{LO,k})\right]^i$$

corresponding equation for the emf is:
for temperatures in subrange k. This equation can be equivalently written as a simple polynomial in each subrange:
Least-squares fits obtained for functions with zero, one, or two internal breakpoints demonstrated that good fits of high statistical quality could be obtained in all three cases. For similar numbers of independent parameters in the functional form, little statistical difference was seen between the different cases or for different choices of breakpoint temperatures. A sample of the functional forms

$$E = b_0 + \sum_{i=1}^{N_k} b_i \; t_{90}^{\;i} \, .$$

considered is presented in Table 3. The order of each polynomial segment was increased until further increases showed no statistically significant reductions in the chi-square value. For a fit with 130 degrees of freedom, a reduction in the reduced chi-square statistic of 1/130 ≈ 0.01 is marginally statistically significant. The values obtained for the reduced chi-square statistic were in most cases significantly less than one, indicating that either we have overestimated the uncertainties of the data or that there are correlations in the data such that the scatter in the data is less than the overall uncertainty. In fact, the model of the correlation of errors that we describe in Section 8 predicts a reduced chi-square value of 0.72, which is close to the observed minimum value of 0.56.

From the models that gave reduced chi-square values of 0.57 or smaller, we chose as the basis of the reference function the spline model with an 8th order polynomial segment from 0 °C to 660.323 °C and a 6th order polynomial segment from 660.323 °C to 1500 °C, which we label the 8/6 model. At the highest temperatures, this model has the advantage that the second and third derivatives of the emf are very smooth and physically plausible. As shown in Figure 6, d^3E/dt^3 does not undergo any unusual fluctuations near 1500 °C, and the values of d^3E/dt^3 are intermediate to those of two other plausible and statistically valid models. At temperatures above 1064 °C, the spread in emf values between different models with similar values of the chi-square statistic is approximately 1.2 μV at

1200 °C and 2 μV at 1500 °C. Examples of this spread are shown in Figure 7. This spread in emf values is small compared to the uncertainty of the reference function, described in Section 8. Residuals of the data from the 8/6 model are shown in Figure 4 for the contact thermometry data and in Figure 5 for the radiometric data. There are small systematic differences between the fixed-point data, the comparison data against the SPRT and the Au/Pt thermocouples, and the comparison data against a radiation thermometer, but in each case the differences are well within the uncertainties of the data.

The tested thermocouples have a small, but nonzero, emf at the ice point primarily as a consequence of differences in the thermoelectric properties of the hot and cold ends of the thermocouples. This was expected based on the measured changes in the thermocouple emf during the 500 h stabilization heat treatment, as shown in Figure 1. The constant term was subtracted from the spline function obtained in the least squares fitting process to create a reference function with an emf of zero at 0 °C. Coefficients of the resulting reference function are shown in Table 4, for use in (2) using reduced temperature as the independent variable, and in Table 5, for use in (3) using temperature in degrees Celsius.

The emf values of the reference function, as well as first and second derivatives, at various fixed-point temperatures are given in Table 6. An inverse function, giving temperature as a function of emf, was derived from the reference function by doing a least squares fit to a set of emf and temperature pairs generated from the reference function. To produce an inverse function with an accuracy commensurate with the accuracy of the reference function, the points were weighted by the uncertainty in temperature equivalent to the standard emf uncertainties given in Table 10. The inverse function has the form

$$t_{90} = c_0 + \sum_{i=1}^{N_k} c_i E^i .$$

Coefficients for the inverse function are shown in Table 7, and the error of the inverse function is shown in Figure 8.

8. Uncertainty of the reference function

The uncertainty of the reference function is a quantitative measure of the probable deviation of the obtained reference function from the true emf-temperature relationship characterizing the tested thermocouples. If the errors of each datum point are uncorrelated, the uncertainty of the reference function will be substantially less than the uncertainty of each datum point, because the number of degrees of freedom in the least squares fit is quite high. If the errors of each datum point are strongly correlated with errors of other data points, however, there will be little reduction in the uncertainty of the reference function from statistical averaging.

To determine the uncertainty of the reference function, we have used Monte Carlo simulation methods [23]. In the numerical simulation, the error of each datum point was assumed to be the linear sum of a set of error subcomponents, each corresponding to one of the uncertainty subcomponents listed in Table 2. Knowledge of the origin of each subcomponent of the combined uncertainty enabled us to make reasonable assumptions about the correlations of errors. For example, an error in the calibration of the SPRT will affect all of the data points obtained in the stirred liquid baths in a correlated manner. We developed a simple model of the error correlations in which each error subcomponent for a particular datum point is either completely correlated or completely uncorrelated with the corresponding component of some subset of the other data points. The model assumed that errors corresponding to thermocouple reproducibility were uncorrelated and that all remaining components were correlated. Treating such errors as bath gradients as completely correlated is pessimistic, however. Consequently, we believe that the model will give a somewhat conservative estimate of the uncertainty of the emf-temperature relationship of the JM93 lot of thermocouples.

A set of 600 model data sets was generated with randomly assigned errors consistent with the correlation model and with standard deviations at each temperature equal to the combined standard uncertainty for that point. A spline polynomial of the same form as the reference function was fitted to each model data set, and the resulting polynomial was evaluated at a set of temperatures. A statistical analysis of the distribution of emf values was used to determine the uncertainty of the reference function. There are two different ways to define the uncertainty of the reference function at a given confidence level, and we now discuss each way in turn.

The first method examines only the distribution of emf values at each temperature. The standard deviation of these values at each temperature was multiplied by a coverage factor of two to obtain the expanded uncertainty of the reference function on a point-by-point basis, which we denote $U_p = 2u_p$. This result is shown as the solid line in Figures 9 and 10. For reference purposes, the expanded uncertainties of the individual data points of Table 10 are shown as crosses in the same figures, and the results of an analysis of U_p with no correlations between uncertainty subcomponents are shown as the dashed lines. Intuitively, one expects the correlated model to give values of U_p less than the expanded uncertainty of individual points (the case of no statistical averaging) and greater than the expanded uncertainty calculated with no correlations (the case of maximal statistical averaging). The position of the solid lines in Figures 9 and 10, intermediate between the dashed lines and the crosses, confirms this intuition.

With this first definition of the uncertainty of the reference function, the probability of the reference function agreeing with the true emf-temperature relationship at any one temperature within the amount U_p is 95%, assuming a normal distribution of errors. Because the reference function covers a broad range of temperatures, there is a substantial probability that the reference function will deviate from the true emf-temperature relationship at some set of temperatures by more than the expanded uncertainty U_p.

The second method of determining the uncertainty considers the reference function as a whole: a confidence or uncertainty band for the reference function will be determined such that, with a certain level of confidence, the reference function does not deviate from the true emf-temperature relationship by more than the width of the confidence band at any temperature. A typical method of analytical statistics to determine this uncertainty is that of Working-Hotelling confidence bands [24]. In this paper, we instead determined the confidence bands numerically [23]. To begin, the values of u_p at an array of temperature values were multiplied by a constant factor, w. Each of the 600 polynomials representing the best fit of each model data set was evaluated at the array of temperature values, and the fraction of polynomials that had errors less than $\pm\ wu_p$ at all temperatures was calculated. This analysis revealed that with a value of w=3.0, 95% of the polynomials lie within the confidence bands $\pm wu_p$ at all temperatures in the range 0 °C to 1500 °C. This confidence band for the reference function treated as a whole is shown as the dash-dot lines in Figures 9 and 10.

The choice of the appropriate uncertainty band will depend on the application of the reference function. Typically, the uncertainty of the reference function will be included as a subcomponent of the combined uncertainty of a thermocouple calibration. Because the uncertainty of thermocouple calibrations is almost always reported as the uncertainty at a single point or temperature value, it is most appropriate in this case to use U_p, shown as the solid lines in Figures 9 and 10, as the expanded uncertainty of the reference function.

As a check on the reference function, a comparison test over the range 720 °C to 1500 °C was performed at NIST between a calibrated type S thermocouple and one of the Pt/Pd thermocouples prepared for this study. The emf of the type S thermocouple was measured at the fixed points of ice, Zn, Al, Ag, and Au, and a calibration equation was obtained by fitting a quadratic function [5] to the deviation of the emf values from the type S reference function. The quadratic function was extrapolated linearly above 1064 °C to 1500 °C. Because the type S thermocouple was fabricated from the same lot of wire used in the redetermination of the type S reference function on the ITS-90 [25], the thermocouple was a close match to the reference function. The maximum deviation of the thermocouple from the reference function was the equivalent of 0.6 K at 1500 °C. The Pt/Pd thermocouple was calibrated as discussed in Section 9. Prior to the comparison test a common measuring junction was constructed in the same manner as described in Section 3.1. The Pt expansion coils of the two thermocouples were removed, the thermoelements were extended by 1.5 cm long lengths of 0.12 mm diameter Pt, Pd, or Pt-10%Rh wires, and these wires were welded into a single common measuring junction. The thermocouple assembly was inserted into a horizontal tube furnace, and emf readings of both thermocouples were made at set of temperatures over the range 720 °C to 1500 °C. Data were taken with increasing temperature. The emf readings of both thermocouples were converted to temperature using the appropriate calibration equations. The difference of the temperature indicated by the type S thermocouple from that indicated by the Pt/Pd thermocouple varied smoothly and monotonically from +0.07 K at 720 °C to -0.37 K at 1500 °C. Studies of thermocouple calibrations at NIST [4,5] have shown that thermocouple calibrations that use a type S thermocouple calibrated at fixed points in a separate apparatus as a reference thermometer have an expanded uncertainty of approximately 0.3 K, up to temperatures of 1100 °C. At the higher temperatures, the expanded uncertainty of the Pt/Pd reference function is about 0.3 K, and there are additional uncertainties of approximately the same magnitude from the extrapolation of the deviation function for each thermocouple and from the uncertainty of the type S reference function. The observed differences between temperatures indicated by the type S and Pt/Pd thermocouples are smaller than the combined measurement uncertainty. This test shows that the type S reference function and the NIST/IMGC Pt/Pd reference function are consistent at temperatures up to 1500 °C.

9. Calibration of Pt/Pd thermocouples using the reference function

Figure 11 shows the deviation of the emf values measured for thermocouples JM93-14, JM93-11, and JM93-2 from the reference function. Each solid line in the figure is a linear function that is a least-squares fit to the emf deviation. The resulting reduced chi-square values of 0.55 for JM93-14, 0.92 for JM93-2, and 0.59 for JM93-11, indicate that the linear function adequately models the deviation of these thermocouples from the reference function over the range of measured temperature points, 0 °C to 1064 °C. At higher temperatures, the agreement of the IMGC data for the four different thermocouples studied by radiometric comparison methods shows that the reference function adequately describes the emf-temperature relation for all thermocouples constructed from the JM93 lot of wire.

As an additional check on the utility of the reference function, we have calibrated at the fixed points of ice, In, Sn, Zn, Al, Ag, and Au three thermocouples constructed from Pd wire of the same or substantially lower purity than the Pd wire used for the thermocouples that form the basis of the reference function. The deviations of the emf values at the fixed points from the reference function for these thermocouples are shown in Figure 12. The deviations at the fixed points for the thermocouple designated JM92-5, made from Pd wire of the same nominal purity as JM93, could be modeled with a linear function. Thermocouples SC89-10 and E90-3, constructed of lower purity Pd of mass fraction ≤99.98 %, required a function of third order when fitted to the deviations at the fixed points. Table 8 gives the weighted rms residuals of the measured emf values from the sum of the reference function and the polynomial deviation function.

There is a lack of practical fixed points in the temperature range from 1084.62 °C (Cu) to 1500 °C. Consequently, it would be highly convenient to be able to extrapolate a calibration performed only up to temperatures of the Au or Cu freezing point. We have investigated the error of extrapolating a calibration by two methods. The first method is mathematical: the difference between the chosen deviation function and a deviation function of one order lower can be taken as an estimate of the error of extrapolation. For thermocouples E90-3 and SC89-10, the differences are the equivalent of 0.34 K and 0.22 K at 1500 °C, respectively. These differences are comparable to the expanded uncertainty of the reference function at 1500 °C, 0.3 K.

The second method consisted of performing comparison measurements between Pt/Pd thermocouples from the set used for determination of the reference function and the thermocouples JM92-5, SC89-10, and E90-3 that had previously been calibrated at fixed points with emf values above 1064 °C obtained by extrapolation. For these tests, a common measuring junction was constructed in the same manner as described in Section 3.1. The Pt expansion coils of the Pt/Pd thermocouples were removed, the thermoelements were extended by 1.5 cm long lengths of 0.12 mm diameter Pt and Pd wires, and these wires were welded into a single common measuring junction. The assembled bundle of thermocouples was inserted at an immersion of 36 cm into the bore of a furnace with a tubular SiC heater [4] that contained a high-purity alumina protection tube of 1.8 cm inner diameter. The first test compared the Pt/Pd thermocouple JM93-14 against JM92-5, SC89-10, and E90-3. Results of this comparison test are shown as the open symbols in Figure 12. After completion of these tests, all of the thermocouples were calibrated against JM93-15 in the same furnace at the same immersion. This second test, performed over the temperature range

660 °C to 1100 °C, checked for any changes in the emf-temperature relationship of either JM93-14 or the test thermocouples. There are two main conclusions from the test:

1. Extrapolation of the fixed-point calibrations introduces an additional error at high temperatures that is smaller than the expanded uncertainty of the reference function.
2. After heating to 1500 °C, small, irreversible changes were detected in the emf-temperature relationship of the thermocouples at lower temperatures, as shown in Table 9. The magnitude of the changes, equivalent to 0.05 K to 0.17 K in the range 660 °C to 1100 °C, is several times larger than the calibration uncertainty of a Pt/Pd thermocouple at temperatures below 1100 °C. Thermocouple JM93-14 changed by less than 50 mK, even without annealing, which is consistent with the *in situ* drift tests performed at IMGC, to be described in Section 10. Measurements of the Pt thermoelements against the Pt of JM93-15 showed minimal changes after heating to 1500 °C, an indication that the changes in the emf of the thermocouples were caused predominantly by changes in the Pd thermoelements.

Because the thermoelectric properties of the Pd thermoelements may significantly change after exposure to high temperatures, we recommend that Pt/Pd thermocouples used at temperatures exceeding 1200 °C should not be used for work of the highest accuracy at lower temperatures.

10. Stability data at high temperatures

After all of the work for the determination of the reference function was complete, an *in situ* drift test was performed at IMGC at temperatures of 1400 °C and 1500 °C. For the initial test at 1400 °C, thermocouple JM 93-11 was aged in the blackbody furnace described in Section 3.2, and periodically emf and radiometric measurements were made. For the first 72 h, the thermocouple emf drifted slightly higher in value, by the equivalent of 0.13 K after 72 h. After 167 h of aging, the furnace was slightly reconfigured when a heater failed. For the next 301 h, the emf varied by not more than the equivalent of -0.17 K. The magnitude of these drifts is comparable to the standard repeatability of the measurements at 1400 °C, u = 0.16 K. Results of this test are shown in Figure 13.

Following the test at 1400 °C, which lasted a total of 468 h, a second *in situ* test was conducted with thermocouple JM93-11 at a temperature of 1500 °C. This test lasted 701 h and was terminated when a heater failed. The maximum deviation of the emf from the initial emf value was equivalent to not more than 0.28 K, which is slightly higher than the standard repeatability of the measurements at 1500 °C, u = 0.18 K. These results are shown in Figure 14.

A more extensive description of these experiments and the results of drift tests for longer periods will be described in a separate publication.

11. Comparison with other reference functions and summary

Figure 15 displays the deviations of literature data on Pt/Pd thermocouples from the NIST/IMGC reference function.

The measurements of Roeser and Wensel [26] used Pt and Pd wires of unknown purity and unknown annealing technique, and at the time of the publication, 1941, the accuracy of emf measurements was limited. Consequently, these data have a large but unknown uncertainty.

At a later date, Freeze et al. [15] studied Pt/Pd thermocouples manufactured from Pd wire of purity similar to that of the thermocouples SC89-10 and E90-3 discussed in Section 9. The deviation of the emf values presented by Freeze et al. from the NIST/IMGC reference function is similar to the deviation curves seen for SC89-10 and E90-3 for temperatures below 1200 °C. There is a change in slope in the deviation curve at approximately 1200 °C, with the slope being more negative at temperatures above 1200 °C. Because Freeze et al. used "high-temperature porcelain" insulating tubes rather than high-purity alumina, this change in the deviation curve may be a result of chemical contamination or increasing electrical leakage through the thermocouple insulator, or both. Additionally, the data of Freeze et al. was determined by comparison of the Pt/Pd thermocouples with type S thermocouples that had been calibrated at the fixed points of Au, Ag, Sb, and Zn, with a linear extrapolation of the calibration for temperatures above 1064 °C. Non-linearity of the deviation of the type S reference function used by Freeze from later, more accurate reference functions [25,27] introduced a substantial error in their results for Pt/Pd thermocouples for temperatures above about 1300 °C. Correcting for this error would increase the emf values given by Freeze et al. by approximately 35 μV at 1400 °C, with the result that the change in slope of the deviation curve near 1200 °C would be reduced by approximately a factor of two.

Two Pt/Pd thermocouples (Pt-Pd1 and Pt-Pd2) documented in the work of Rhee et al. [28] were constructed from Pd of the same nominal purity as the JM92 and JM93 lots of Pd described here. The emf values measured at a series of fixed points agree well with the values of the NIST/IMGC reference function, with the exception of the emf at the indium freezing point, which has a deviation in emf that is more negative than that of the other fixed points. The deviations of the results of Edler et al. [12] and of Freeze et al. [15] do not show a dip near the In freezing point, so we suspect there is a problem with the data of Reference [28] at this point.

Crovini et al. [11] reported comparisons of type S thermocouples with Pt/Pd thermocouples manufactured from wire obtained from several manufacturers. Their results indicate that emf deviations that are either positive or negative with respect to the NIST/IMGC reference function are possible, depending on the relative purities and types of impurities of the Pt and Pd legs. The thermocouple JM1 discussed in Reference [11] was constructed from Pt and Pd of the same nominal purity as the thermocouples used in the determination of the NIST/IMGC reference function, and the agreement with the reference function is quite good over the range of data for JM1.

The work reported by Pokhodoun et al. [16] utilized a novel Pt/Pd thermocouple whose measuring junction was integral with the back wall of a Pd blackbody cavity. The radiometry results of Reference [16] differ significantly from that of the present work. At a temperature near 1200 °C, the data show a large change in the slope of the emf deviation from the NIST/IMGC reference function. Because the thermocouples studied by Pokhodoun et al. were mounted in alumina insulators, which have low electrical conductance at 1200 °C, this effect does not appear to be a consequence of electrical leakage through the insulators. It is unlikely that this effect is a result of differences in the Pd composition between the JM93 thermocouples and the thermocouples tested by Pokhodoun et al., because no similar effect was observed in our comparison tests of the Pt/Pd thermocouples JM92-5, SC89-10, and E90-3 against thermocouples from the JM93 lot, described in Section 9.

The work of Pokhodoun et al. [16] additionally suggests that Pt/Pd thermocouples may be calibrated at a small number of points and a calibration curve obtained by a direct fit of the emf-temperature data pairs, rather than a fit of the deviation of the emf from a reference function. This procedure results in an emf-temperature relationship with a strongly temperature-dependent deviation from the NIST/IMGC reference function in the temperature range between 660 °C and 900 °C, as seen in Figure 15 where the polynomial labeled Variant G [16] has been plotted. The absence of data in this range indicates that this structure is a mathematical artifact and is not physical. The excellent results that we have obtained for the calibration of thermocouples JM92-5, SC89-10, and E90-3 demonstrate that far greater accuracy may be achieved by a least-squares fit to the emf deviation from the reference function.

Edler et al. [12] give three possible reference functions for Pt/Pd thermocouples over the temperature range 0 °C to 1084 °C. The results for their thermocouple 9/90 are shown in Figure 15. The deviation of the emf of this thermocouple is very close to a linear function of temperature, similar to what was found for thermocouples SC89-10 and E90-3 discussed in Section 9.

The most accurate reference function or tabular data from the literature is that of Edler et al. [12], with quoted uncertainties of 80 mK at 200 °C, 45 mK at 600 °C, and 30 mK at 1000 °C. The uncertainties of the NIST/IMGC reference function are a factor of three to a factor of eight smaller. Additionally, the high upper temperature limit of 1500 °C of the NIST/IMGC reference function and the demonstrated stability of Pt/Pd thermocouples at this temperature make the reference function presented here valuable for high temperature use of Pt/Pd thermocouples.

Acknowledgments

We thank Will Guthrie of the NIST Statistical Engineering Division for his helpful advice on statistics.

References

*Identification of commercial equipment and materials in this paper does not imply recommendation or endorsement by the National Institute of Standards and Technology, nor does it imply that the equipment and materials identified are necessarily the best available for the purpose.

1. *Manual on the Use of Thermocouples in Temperature Measurement*, 4th Ed., ASTM Manual Series: MNL 12, Philadelphia, ASTM, 1993, 290 p.
2. *Guide to the Expression of Uncertainty in Measurement*, Geneva, ISO, 1993, 101 p.
3. Jones T. P., *Metrologia*, 1968, **4**, 80-83
4. Burns G. W., Scroger M. G., *NIST Measurement Services: The Calibration of Thermo-couples and Thermocouple Materials*, NIST Special Publication 250-35, Washington, D.C., U. S. Government Printing Office, 1989, 201 p.
5. Ripple, D., Burns, G. W., Scroger M. G., *Assessment of Uncertainties of Thermocouple Calibrations at NIST*, NISTIR 5340, Gaithersburg, MD, NIST, 1994, 34 p.

6. McLaren E. H., Murdock E. G., In *Temperature: Its Measurement and Control in Science and Industry*, Vol. 4 (Edited by H. H. Plumb), Pittsburgh, PA, Instrument Soc. America, 1972, 1543-1560
7. McLaren E. H., Murdock E. G., In *Temperature: Its Measurement and Control in Science and Industry*, Vol. 5 (Edited by J. F. Schooley), New York, American Institute of Physics, 1982, 953-975
8. Bentley R. E., Jones T. P., *High Temperatures — High Pressures*, 1980, **12**, 33-45
9. McLaren E. H., Murdock E. G., *The Pt/Au Thermocouple, Part I: Essential Performance, Part II: Preparatory Heat Treatment, Wire Comparisons and Provisional Scale*, Ottawa, National Research Council of Canada Publication NRCC/27703, 1987
10. Burns G. W., Strouse G. F., Liu B. M., Mangum B. W., In *Temperature: Its Measurement and Control in Science and Industry*, Vol. 6 (Edited by J. F. Schooley), New York, American Institute of Physics, 1992, 531-536
11. Crovini L., Actis A., Fernicola V., Galleano R., In *Report to the 18th Meeting of the CCT*, paper CCT/93-17, 1993
12. Edler F., Jung H. J., Maas H., Le Pommelec J. Y., In *Report to the 18th Meeting of the CCT*, paper CCT/93-5, 1993
13. Burns G. W., Ripple D. C., In *Proceedings of TEMPMEKO `96, 6th International Symposium on Temperature and Thermal Measurements in Industry and Science*, Torino, Italy, Levrotto & Bella, 1997, 171-176
14. Battuello M., Ali K., Girard F., In *Proceedings of TEMPMEKO `96, 6th International Symposium on Temperature and Thermal Measurements in Industry and Science*, Torino, Italy, Levrotto & Bella, 1997, 177-182
15. Freeze P. F., Caldwell F. R., Davis E. R., *Reference Tables for the Palladium vs. Platinum-15% Iridium Thermocouple*, Technical Documentary Report No. ASD-TDR-62-525, Washington, Nat. Bur. Stds., 1962, 77 p.
16. Pokhodoun A. I., Matveyev M. S., Bonnier G., Ronsin H., In *Report to the 19th Meeting of the CCT*, paper CCT/96-34, 1996
17. Powell R. L., Sparks L. L., Hust J. G., *Standard Reference Materials: Standard Thermocouple Material, Pt-67: SRM-1967*. Natl. Bur. Stand. (U.S.) Special Publ. 260-56, Washington, D.C., U. S. Govt. Printing Office, 1978, 50 p.
18. Mangum B. W., *Reproducibility of the Temperature of the Ice Point in Routine Measurements*, NIST Technical Note 1411, Washington, D.C., U. S. Government Printing Office, 1995, 24 p.
19. Preston-Thomas H., *Metrologia* 1990, **27**, 3-10. *ibid*., 107
20. Marcarino P., Dematteis R., Tiziani A., In *Proceedings of IMEKO XIII*, Vol. 2, Turin, 1994, 1377-1382
21. Battuello M., Lanza F., Ricolfi T., *Metrologia*, 1990, **27**, 75-82
22. Battuello M., Ricolfi T., Wang L., *Metrologia*, 1995/96, **32**, 371-378
23. Press W. H., Flannery B. P., Teukolsky S. A., Vetterling W. T., *Numerical Recipes*, Cambridge, Cambridge University, 1986, p. 529
24. Neter J., Wasserman W., Kutner, M., *Applied Linear Regression Models*, Homewood, Illinois, Richard D. Irwin, Inc., 1983, p. 244
25. Burns G. W., Strouse G. F., Mangum B. W., Croarkin M. C., Guthrie W. F., Marcarino P., Battuello M., Lee H. K., Kim J. C., Gam K. S., Rhee C., Chattle M., Arai M., Sakurai H.,

Pokhodoun A. I., Moiseeva N. P., Perevalova S. A., de Groot M. J., Zhang J., Fan K., S. Wu, In *Temperature: Its Measurement and Control in Science and Industry*, Vol. 6 (Edited by J. F. Schooley), New York, American Institute of Physics, 1992, 537-546

26. Roeser W. F., Wensel H. T., In *Temperature: Its Measurement and Control in Science and Industry*, New York, Reinhold, 1941, 1293-1323
27. Bedford R. E., Ma C. K., Barber C. R., Chandler T. R., Quinn T. J., Burns G. W., Scroger M., In *Temperature: Its Measurement and Control in Science and Industry*, Vol. 4 (Edited by H. H. Plumb), Pittsburgh, Instrument Soc. America, 1972, 1585-1602
28. Rhee C., Chi D., Kang K. H., Gam K. S., Kim Y. G., Hahn J. W., Park S. N., In *Report to the 18th Meeting of the CCT*, paper CCT/93-31, 1993

Table 1. Spectrochemical analysis of the JM93 Pd wire.

Element	(Mass fraction)$\times 10^6$
Ca	<1
Cu	3
Au	<1
Fe	1
Mg	<1
Mn	3
Pt	<10
Si	5
Ag	<1

Table 2. Summary of the subcomponents of uncertainty of the data, expressed as the standard uncertainty of the emf in microvolts. Subcomponents that refer to an uncertainty of temperature, such as the SPRT calibration, have been converted to equivalent uncertainties of emf.

NIST Measurements		$u_i\,/\mu$V	
Type A		minimum	maximum
	Repeatability of Pt/Pd TCs	0.018	0.069
	Oxidation drift of Pt/Pd TCs	0.00	0.21
Type B			
	Uncertainty of emf measurements	0.010	0.059
	Bath gradients and stability	0.016	0.030
	SPRT calibration	0.001	0.005
	Au/Pt TC calibration	0.029	0.15
	Au/Pt TC repeatability	0.016	0.057
	Inhomogeneity of Pt/Pd TCs	0.000	0.047
	Uncertainty of fixed point temperature	0.003	0.10
IMGC Measurements			
Type A (Type B for 1350 °C to 1500 °C)			
	Repeatability of TCs and radiometry	0.8	4.5
Type B			
	Radiation thermometer calibration	0.50	1.5
	Size of source effect	0.17	1.0
	Emissivity	0.17	1.0
	Uncertainty of voltage measurements	0.50	0.8
	Fixed-point measurement uncertainty (combined)	0.10	0.20

Table 3. Statistical results for the least-squares fit to the data for several spline and polynomial models. The orders of the polynomials for each subrange are listed from the lowest temperature subrange to the highest. The 8/6 spline model with a breakpoint at 660.323 °C is the basis for the NIST/IMGC reference function. A freezing point is denoted as FP.

Orders of polynomials for each subrange	Temperature values for breakpoints	Reduced chi-square value	Degrees of freedom
9	none	0.93	132
10	none	0.56	131
11	none	0.56	130
6/7	419.527 °C (Zn FP)	0.59	130
7/6	660.323 °C (Al FP)	0.60	130
8/5	660.323 °C (Al FP)	0.68	130
8/6	660.323 °C (Al FP)	0.57	129
8/7	660.323 °C (Al FP)	0.57	128
6/5/4	419.527 °C (Zn FP), 1064.18 °C (Au FP)	0.57	130
6/6/5	419.527 °C (Zn FP), 1064.18 °C (Au FP)	0.57	128

Table 4. Coefficients, a_i, of the NIST/IMGC reference function for Pt/Pd thermocouples. The function gives the thermoelectric voltage, E, in microvolts as a function of reduced temperature, t_R, for the indicated temperature ranges. The reduced temperature is defined as $t_R = (t_{90} - t_{LO})/(t_{HI} - t_{LO})$, where t_{HI} and t_{LO} are the upper and lower limits, respectively, of the temperature subrange. See (2).

Temperature Range:	0 °C to 660.323 °C	660.323 °C to 1500 °C
a_0 =	0.000	5782.382
a_1 =	3497.703	11 734.683
a_2 =	2010.298	6713.591
a_3 =	-2764.669	-480.429
a_4 =	5688.825	-2090.249
a_5 =	-2526.521	1747.312
a_6 =	-1051.559	-475.638
a_7 =	1235.904	
a_8 =	-307.599	

Table 5. Coefficients, b_i, of the NIST/IMGC reference function for Pt/Pd thermocouples. The function gives the thermoelectric voltage, E, in microvolts as a function of the temperature, t_{90}, in degrees Celsius for the indicated temperature ranges. See (3).

Temperature Range:	0 °C to 660.323 °C	660.323 °C to 1500 °C
b_0 =	0.000 000	$-4.977\,137\,0\times10^{2}$
b_1 =	5.296 958	$1.018\,254\,5\times10^{1}$
b_2 =	$4.610\,494\times10^{-3}$	$-1.579\,351\,5\times10^{-2}$
b_3 =	$-9.602\,271\times10^{-6}$	$3.636\,170\,0\times10^{-5}$
b_4 =	$2.992\,243\times10^{-8}$	$-2.690\,150\,9\times10^{-8}$
b_5 =	$-2.012\,523\times10^{-11}$	$9.562\,736\,6\times10^{-12}$
b_6 =	$-1.268\,514\times10^{-14}$	$-1.357\,073\,7\times10^{-15}$
b_7 =	$2.257\,823\times10^{-17}$	
b_8 =	$-8.510\,068\times10^{-21}$	

Table 6. Thermoelectric values at fixed points and the upper temperature limit for the NIST/IMGC reference function for Pt/Pd thermocouples. A melting point is denoted as MP, a triple point as TP, and a freezing point as FP.

Temperature °C	E μV	dE/dt_{90} μV/K	d^2E/dt_{90}^2 nV/K^2
0.000 (Ice MP)	0.00	5.297	9.22
0.01 (Water TP)	0.05	5.297	9.22
29.764 6 (Ga MP)	161.52	5.549	7.81
156.598 5 (In FP)	921.65	6.429	7.31
231.928 (Sn FP)	1 428.56	7.059	9.61
321.069 (Cd FP)	2 100.54	8.070	13.09
327.462 (Pb FP)	2 152.40	8.154	13.33
419.527 (Zn FP)	2 964.35	9.533	16.46
630.63 (Sb FP)	5 375.83	13.408	19.16
660.323 (Al FP)	5 782.38	13.975	19.04
961.78 (Ag FP)	10 813.09	19.187	14.95
1064.18 (Au FP)	12 853.2	20.631	13.28
1084.62 (Cu FP)	13 277.6	20.899	12.97
1500	22 931.7	25.298	8.71

Table 7. Coefficients of an approximate inverse function for the NIST/IMGC reference function for Pt/Pd thermocouples. The function gives temperature, t_{90}, in degrees Celsius as a function of the thermoelectric voltage, E, in microvolts in selected temperature and voltage ranges. See (4).

Temperature Range:	0 °C to 660.323 °C	660.323 °C to 1500 °C
Voltage Range:	0 μV to 5782.4 μV	5782.4 μV to 22 932 μV
c_0 =	$1.128\,648\,1\times10^{-3}$	1.314 565
c_1 =	$1.886\,785\,0\times10^{-1}$	$1.944\,512\times10^{-1}$
c_2 =	$-3.001\,252\,1\times10^{-5}$	$-2.439\,432\times10^{-5}$
c_3 =	$1.846\,873\,7\times10^{-8}$	$2.735\,961\times10^{-9}$
c_4 =	$-1.249\,860\,8\times10^{-11}$	$-2.131\,711\times10^{-13}$
c_5 =	$5.241\,650\,9\times10^{-15}$	$1.114\,340\times10^{-17}$
c_6 =	$-1.391\,528\,6\times10^{-18}$	$-3.715\,739\times10^{-22}$
c_7 =	$2.387\,290\,8\times10^{-22}$	$7.121\,084\times10^{-27}$
c_8 =	$-2.580\,243\,6\times10^{-26}$	$-5.954\,960\times10^{-32}$
c_9 =	$1.601\,881\,9\times10^{-30}$	
c_{10} =	$-4.360\,816\,6\times10^{-35}$	
Error Range:	-3 mK to 2 mK	-35 mK to 25 mK

Table 8. Results of fitting the emf deviation from the NIST/IMGC reference function of fixed-point data for three Pt/Pd thermocouples. The rms residual is the square root of the sum of the residuals squared divided by the numbers of degrees of freedom.

Thermocouple	Order of Deviation Function	Reduced chi-square	rms residual, in equivalent mK
JM92-5	1	1.22	5.9
JM92-5	2	1.47	7.1
SC89-10	2	18.5	23.6
SC89-10	3	0.63	5.4
E90-3	2	45.6	37.9
E90-3	3	5.3	12.6

Table 9. Equivalent temperature change, measured at 660 °C and 1100 °C, for Pt/Pd thermocouples exposed to temperatures up to 1500 °C.

	Equivalent temperature change / K	
Thermocouple	at 660 °C	at 1100 °C
JM93-14* without annealing	-0.05	-0.05
JM93-14* after annealing	-0.01	-0.04
JM92-5 without annealing	-0.12	-0.06
JM92-5 after annealing	-0.07	-0.04
SC89-10 without annealing	-0.05	0.04
E90-3 without annealing	-0.17	-0.10

*Thermocouple JM93-14 was cycled twice to 1500 °C

Table 10. Experimental values for temperature, t_{90}, thermoelectric voltage, E, and standard combined uncertainty, u_c, used for the derivation of the NIST/IMGC reference function. The values listed are for thermocouple JM93-15, except where noted.

t/°C	E/μV	u_c/μV
SPRT comparison, water bath		
14.971	80.191	0.026
30.000	162.740	0.027
45.055	247.189	0.027
59.990	332.582	0.028
74.768	418.615	0.028
94.928	538.325	0.029
SPRT comparison, oil bath run 1		
94.971	538.663	0.029
115.002	660.269	0.030
134.969	784.198	0.031
154.956	910.994	0.032
174.996	1041.072	0.033
194.993	1173.989	0.034
214.996	1310.287	0.035
235.026	1450.385	0.036
255.027	1594.157	0.037
275.006	1741.960	0.039
SPRT comparison, oil bath run 2		
94.960	538.505	0.019*
114.976	660.104	0.030
134.995	784.330	0.031
154.949	910.937	0.032
174.996	1041.072	0.033
SPRT comparison, salt bath		
275.006	1741.981	0.039
300.003	1933.303	0.040
325.019	2132.439	0.042
349.933	2338.994	0.044
375.046	2556.110	0.046
399.935	2780.669	0.049
424.990	3016.610	0.051
449.944	3262.040	0.054

t/°C	E/μV	u_c/μV
NIST fixed points before comp. runs		
0.000	-0.069	0.021
156.599	921.591	0.024
231.928	1428.509	0.027
419.527	2964.298	0.037
660.322	5782.330	0.058
961.776	10 813.00	0.085
1064.170	12 852.90	0.137
NIST fixed points after comp. runs		
0.000	-0.119	0.021
156.599	921.572	0.024
231.928	1428.499	0.027
419.527	2964.254	0.037
660.322	5782.287	0.058
961.776	10 812.98	0.085
1064.170	12 852.85	0.137
NIST fixed points for JM93-16		
0.000	-0.053	0.021
156.599	921.593	0.030
231.928	1428.517	0.037
419.527	2964.334	0.059
660.322	5782.309	0.058
961.776	10 813.01	0.085
1064.170	12 852.90	0.137
IMGC fixed points for JM93-16		
660.323	5782.40	0.10
961.780	10 813.25	0.20
961.780	10 812.90	0.20

*Multiple measurements at different positions in the bath

$t/°C$	$E/\mu V$	$u_c/\mu V$
Au/Pt 91-10 comp., comparator cell		
419.733	2966.188	0.046
444.370	3206.220	0.049
475.010	3519.261	0.052
505.342	3845.640	0.056
537.117	4205.609	0.060
568.291	4577.167	0.064
598.557	4955.580	0.068
629.795	5364.566	0.072
660.219	5780.842	0.076
696.317	6297.599	0.081
734.154	6865.563	0.087
773.939	7491.224	0.093
813.486	8141.217	0.100
853.714	8830.367	0.119
893.130	9531.870	0.149
933.412	10 274.67	0.185
961.872	10 814.55	0.212
980.186	11 168.41	0.241
998.181	11 520.95	0.272
Au/Pt 94-2 comp., comparator cell		
419.425	2963.253	0.046
445.504	3217.493	0.049
470.471	3471.849	0.052
501.967	3808.459	0.055
539.742	4236.146	0.060
580.298	4725.173	0.065
620.455	5240.265	0.071
660.270	5781.524	0.076
699.803	6348.819	0.082
739.812	6952.774	0.088
780.230	7592.768	0.094
820.581	8260.821	0.102
860.233	8944.713	0.124
900.275	9661.875	0.155
939.086	10 381.40	0.190
961.675	10 810.86	0.212
979.456	11 154.35	0.229
996.081	11 479.64	0.268

$t/°C$	$E/\mu V$	$u_c/\mu V$
Au/Pt 93-1 comp., comparator cell		
419.431	2963.311	0.046
446.387	3226.309	0.049
475.804	3527.577	0.052
505.966	3852.490	0.056
537.556	4210.714	0.060
568.736	4582.576	0.064
598.856	4959.385	0.068
630.236	5370.437	0.072
660.516	5784.960	0.076
696.619	6302.014	0.081
734.509	6871.010	0.087
774.173	7494.988	0.093
813.775	8146.115	0.100
853.981	8835.108	0.120
893.872	9545.434	0.150
930.668	10 223.35	0.182
961.616	10 809.78	0.211
980.793	11 180.38	0.242
998.352	11 524.49	0.278
Radiometric comp., JM93-12		
1001.20	11 581.5	1.41
1050.40	12 570.7	1.48
1099.47	13 593.0	1.56
1148.17	14 630.4	1.65
1197.61	15 719.6	1.76
1249.77	16 895.8	1.83
1298.69	18 025.0	1.91
Radiometric comp., JM93-13		
1001.43	11 585.7	1.41
1050.61	12 575.3	1.48
1099.72	13 594.6	1.56
1149.57	14 661.4	1.65
1197.95	15 726.7	1.76
1249.60	16 891.9	1.83
1298.89	18 030.8	1.91

t/°C	E/μV	u_c/μV
Radiometric comp., JM93-16		
802.04	7952.6	1.11
850.06	8767.9	1.18
900.69	9671.2	1.27
950.71	10 601.9	1.34
1000.50	11 568.0	1.41
1050.05	12 565.1	1.48
1099.86	13 599.1	1.56
1148.06	14 631.3	1.65
1197.56	15 718.2	1.76
1249.59	16 892.0	1.83
1298.69	18 024.2	1.91
Radiometric comp., JM93-11		
1350.95	19 263.6	3.95
1399.70	20 440.4	4.40
1448.43	21 639.3	4.68
1497.81	22 875.1	5.02
Radiometric comp., JM93-12		
1350.14	19 242.8	3.95
1399.32	20 429.7	4.40
1448.25	21 638.8	4.68
1497.53	22 867.8	5.02

Figure Captions

Figure 1. The emf change at the Ag freezing point of the Pt/Pd thermocouples constructed for the NIST/IMGC study, as a function of time of heating in air at 1100 °C.

Figure 2. Schematic of blackbody and furnace used at IMGC for comparison measurements between Pt/Pd thermocouples and a radiation thermometer calibrated on the ITS-90.

Figure 3. Immersion profile of the Pt/Pd thermocouple JM93-15 on insertion into and withdrawal from the Ag freezing-point cell during a freeze.

Figure 4: Deviations of emf values from the 8/6 spline model over the range of the contact thermometry comparison data.

Figure 5. Deviations of emf values from the 8/6 spline model over the range of the radiometric data.

Figure 6. Second and third derivatives of several polynomial or spline models of the data.

Figure 7. Deviations of alternative models of the data from the chosen 8/6 spline model. For temperatures greater than 1080 °C , the plotted values of emf are 10× less than the actual values.

Figure 8. Error of the approximate inverse function.

Figure 9. Expanded uncertainty of the NIST/IMGC reference function for Pt/Pd thermocouples and of the contact thermometry data.

Figure 10. Expanded uncertainty of the NIST/IMGC reference function for Pt/Pd thermocouples and of the radiometric data.

Figure 11. Deviation of data from the NIST/IMGC reference function for Pt/Pd thermocouples JM93-14, JM93-11, and JM93-2 constructed from Pd of 99.997% mass fraction.

Figure 12. Deviation of data from the NIST/IMGC reference function for Pt/Pd thermocouples SC89-10, E90-3, and JM92-5. The lines are polynomial fits to the fixed-point data only.

Figure 13. Results of an *in situ* drift test at 1400 °C of Pt/Pd thermocouple JM93-11 mounted in the apparatus shown in Figure 2, with the IMGC radiation thermometer as the reference thermometer.

Figure 14. Results of an *in situ* drift test at 1500 °C of Pt/Pd thermocouple JM93-11, with the IMGC radiation thermometer as the reference thermometer.

Figure 15. Deviation of data or reference functions obtained from the literature from the NIST/IMGC reference function for Pt/Pd thermocouples.

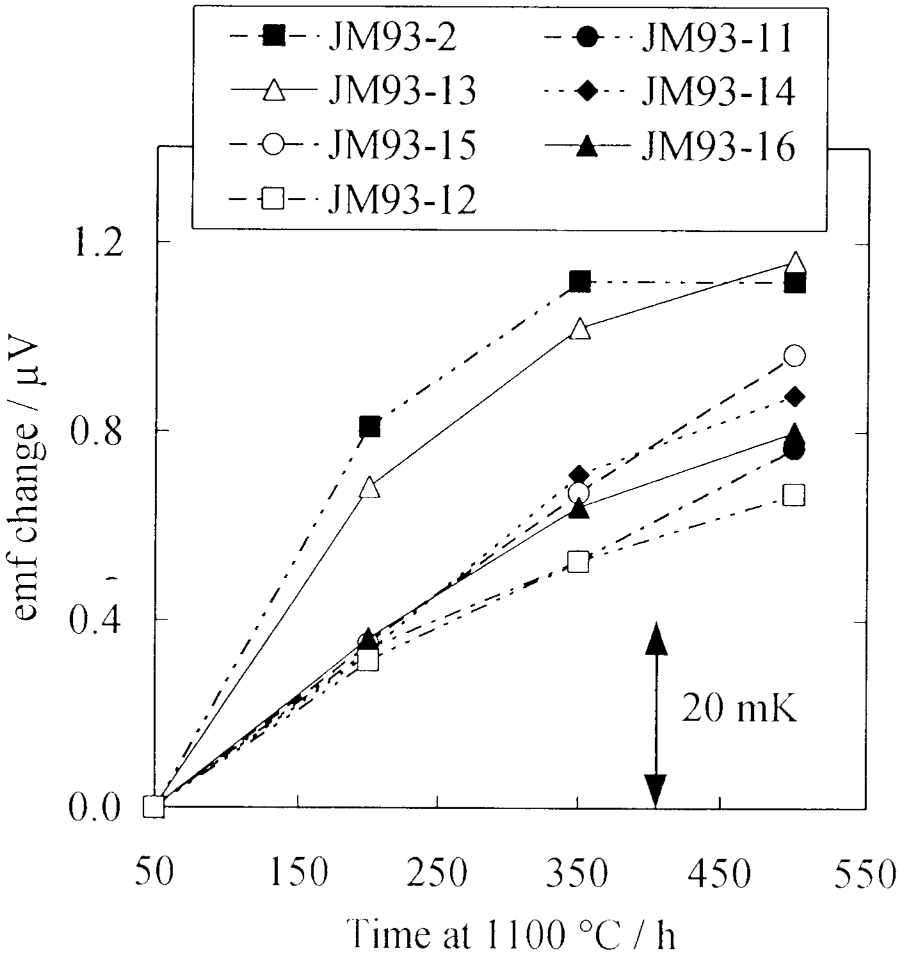
JM93-2
JM93-11
JM93-13
JM93-14
JM93-15
JM93-16
JM93-12
1.2
0.8
0.4
0.0
emf change / µV
20 mK
50
150
250
350
450
550
Time at 1100 °C / h

Fig. 1

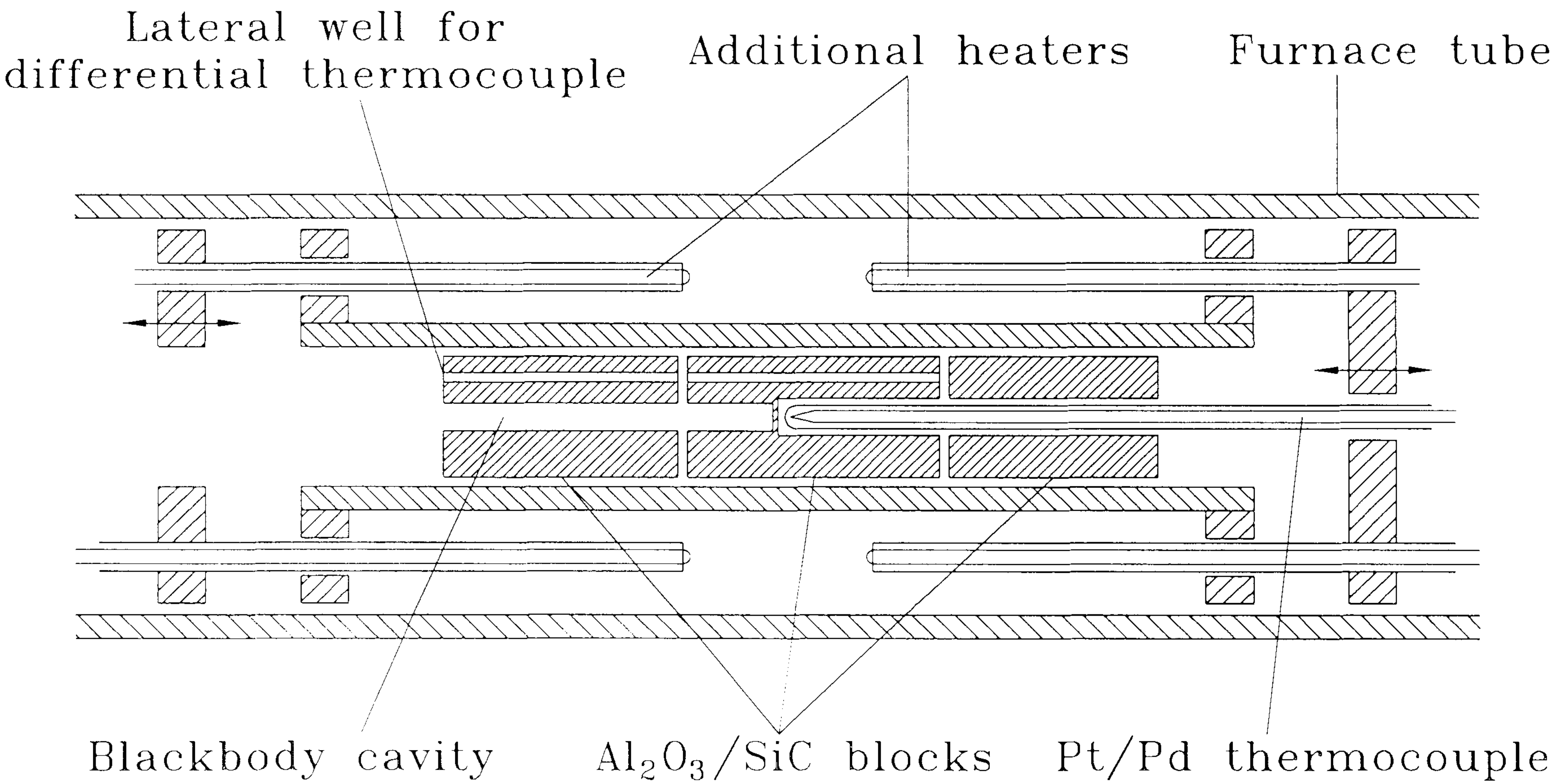
Lateral well for differential thermocouple
Additional heaters
Furnace tube
Blackbody cavity
Al_2O_3/SiC blocks
Pt/Pd thermocouple

Fig. 2

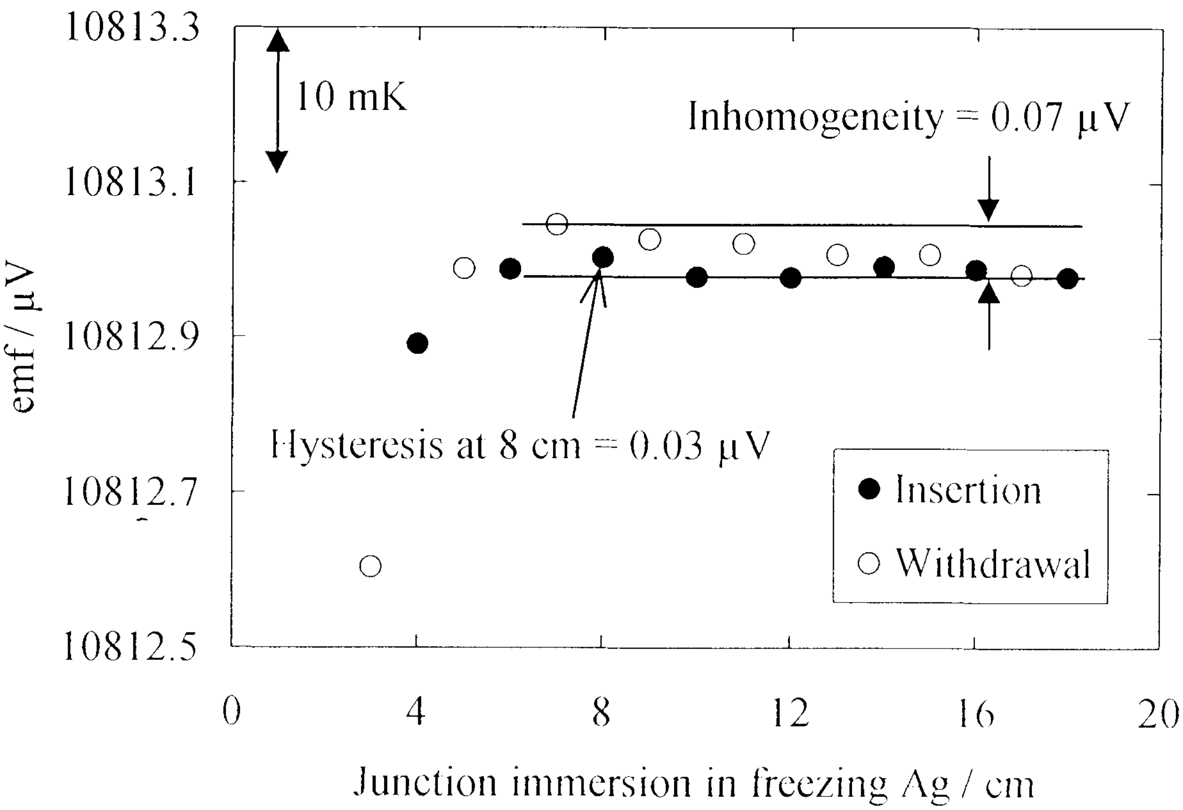
10813.3
10813.1
10812.9
10812.7
10812.5
emf / µV
10 mK
Inhomogeneity = 0.07 µV
Hysteresis at 8 cm = 0.03 µV
Insertion
Withdrawal
0
4
8
12
16
20
Junction immersion in freezing Ag / cm

Fig. 3

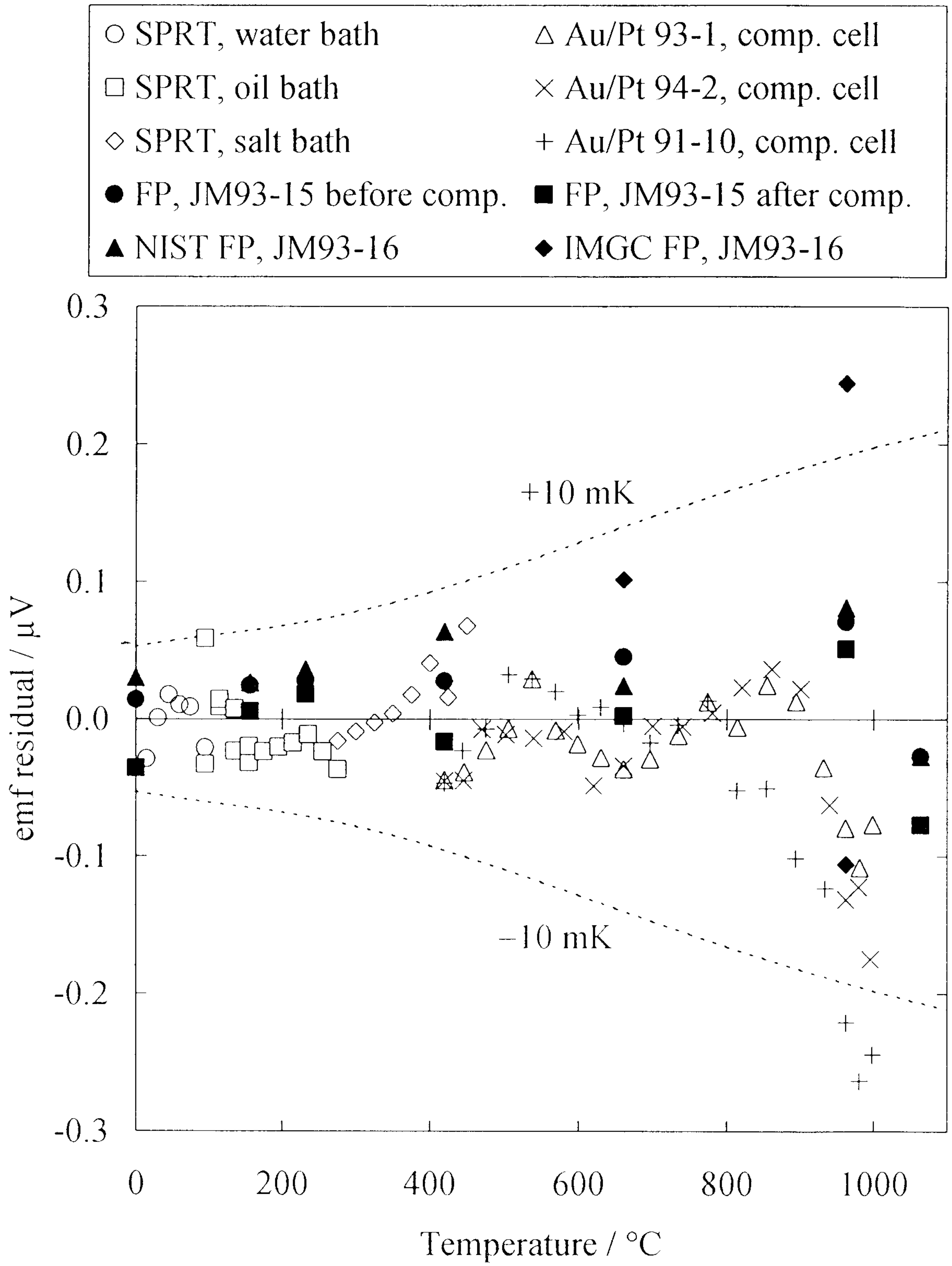
SPRT, water bath
SPRT, oil bath
SPRT, salt bath
FP, JM93-15 before comp.
NIST FP, JM93-16
Au/Pt 93-1, comp. cell
Au/Pt 94-2, comp. cell
Au/Pt 91-10, comp. cell
FP, JM93-15 after comp.
IMGC FP, JM93-16
+10 mK
−10 mK
emf residual / μV
Temperature / °C
0.3
0.2
0.1
0.0
-0.1
-0.2
-0.3
0
200
400
600
800
1000

Fig 4

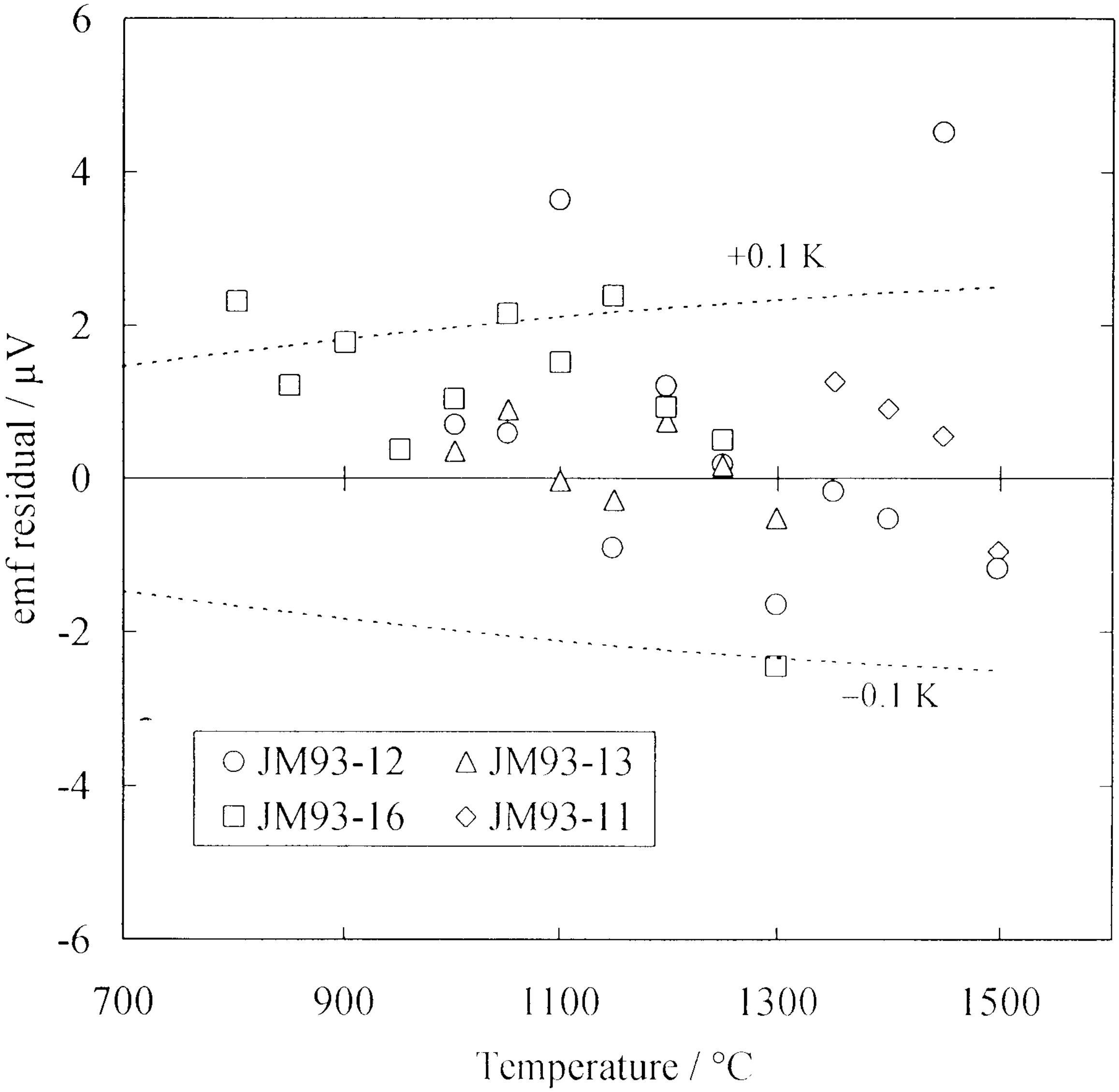
6
4
2
0
-2
-4
-6
emf residual / µV
700
900
1100
1300
1500
Temperature / °C
+0.1 K
−0.1 K
JM93-12
JM93-13
JM93-16
JM93-11

Fig. 5

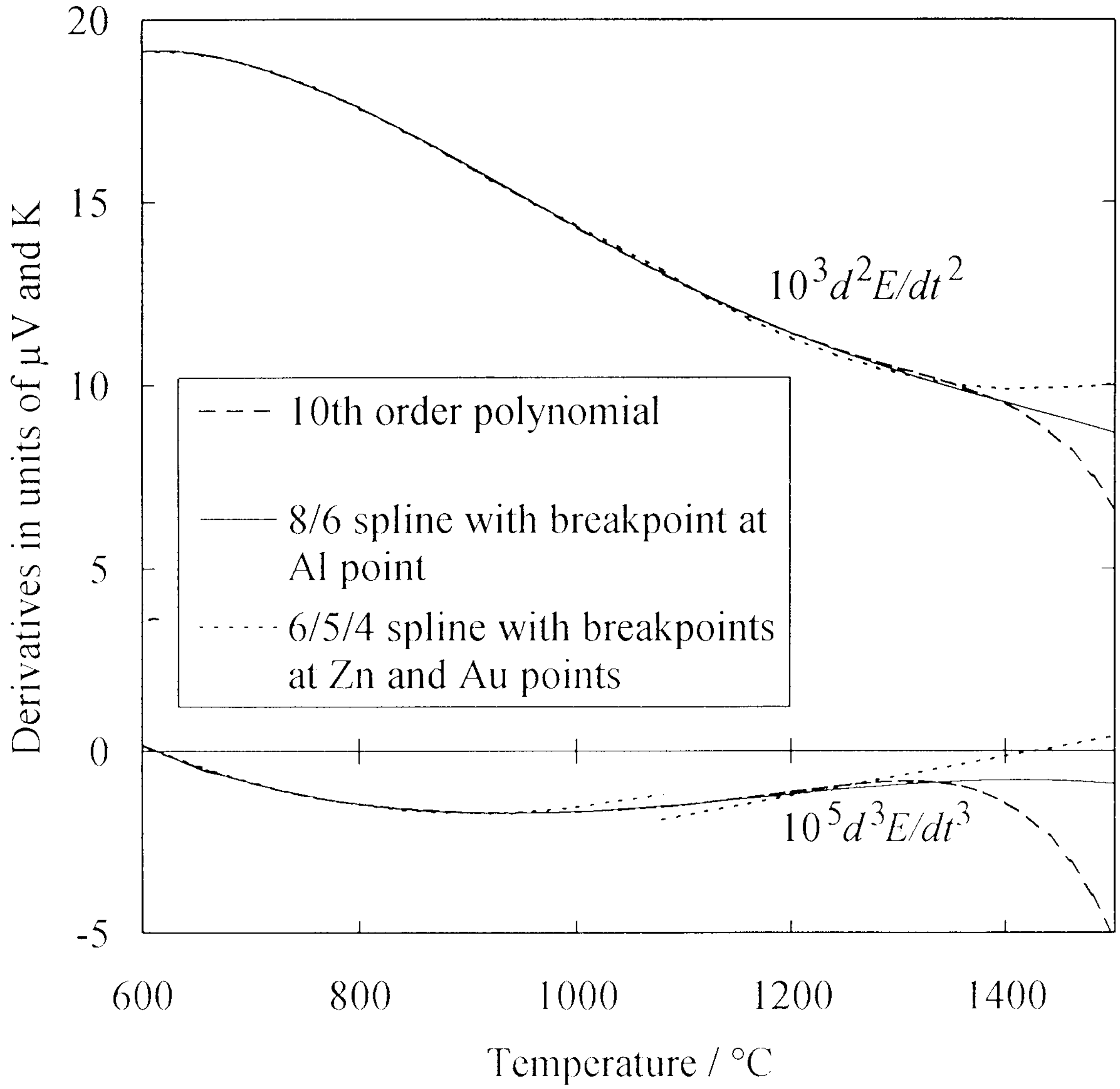
20
15
10
5
0
-5
600
800
1000
1200
1400
Derivatives in units of μV and K
Temperature / °C
$10^3 d^2E/dt^2$
$10^5 d^3E/dt^3$
10th order polynomial
8/6 spline with breakpoint at Al point
6/5/4 spline with breakpoints at Zn and Au points

Fig. 6

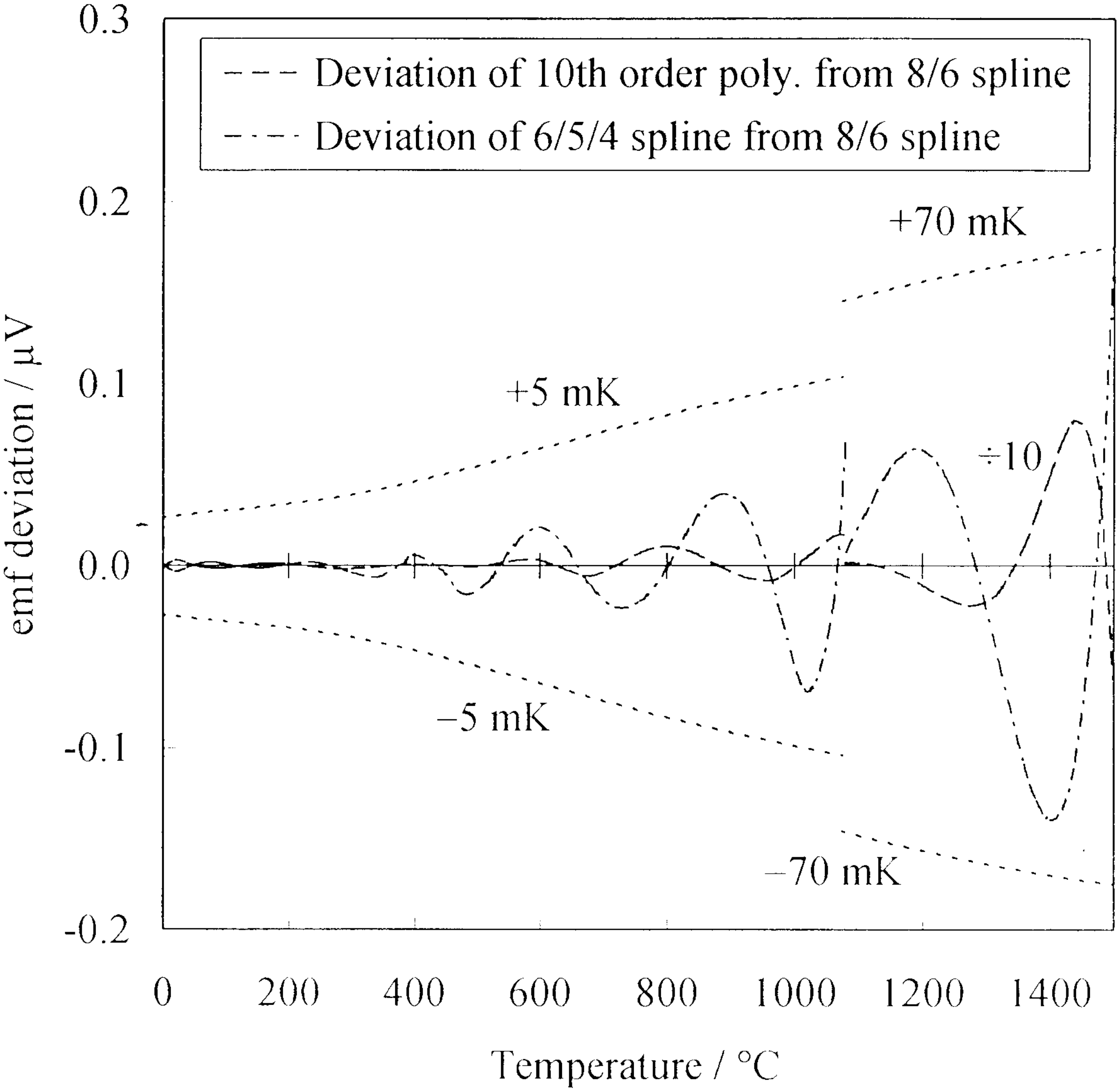

Deviation of 10th order poly. from 8/6 spline
Deviation of 6/5/4 spline from 8/6 spline
+70 mK
+5 mK
÷10
−5 mK
−70 mK
emf deviation / µV
0.3
0.2
0.1
0.0
-0.1
-0.2
0
200
400
600
800
1000
1200
1400
Temperature / °C

Fig. 7

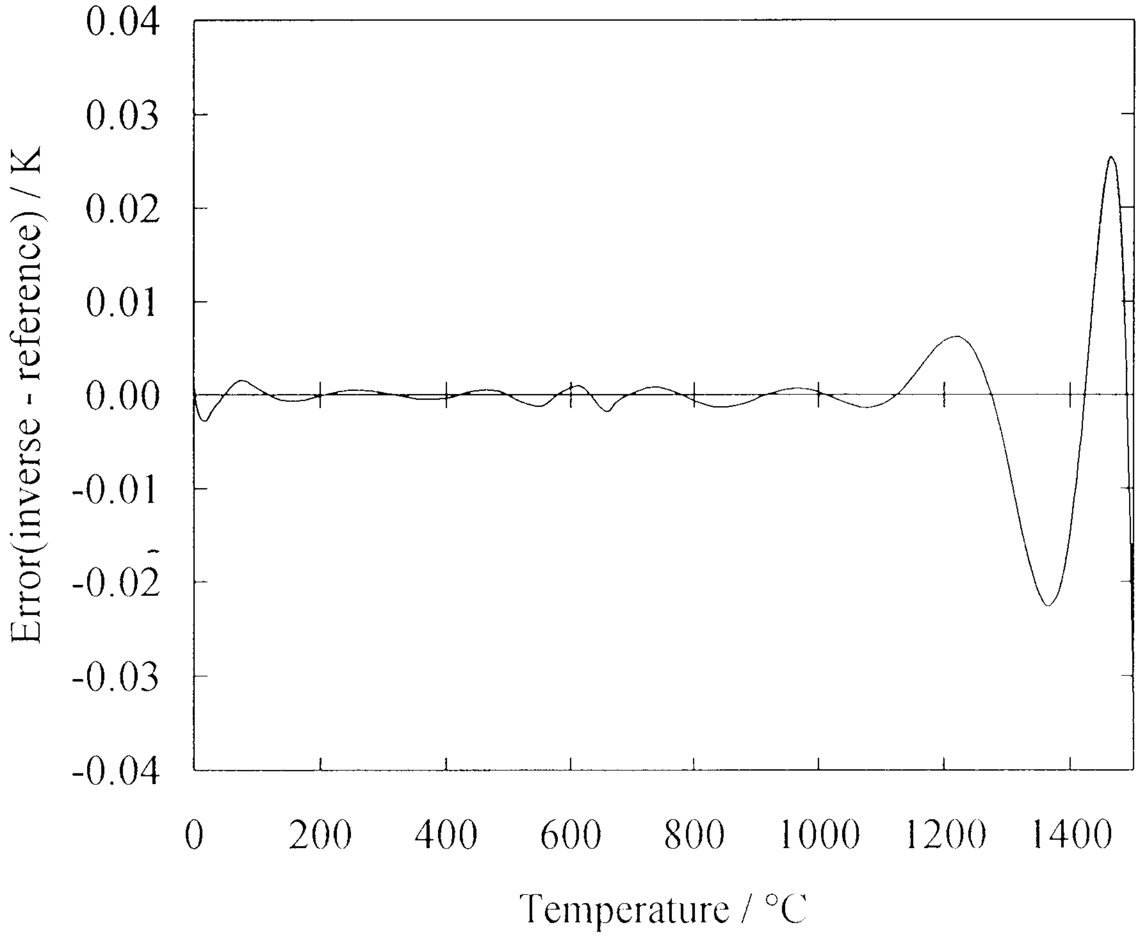
0.04
0.03
0.02
0.01
0.00
-0.01
-0.02
-0.03
-0.04
Error(inverse - reference) / K
0
200
400
600
800
1000
1200
1400
Temperature / °C

Fig. 8

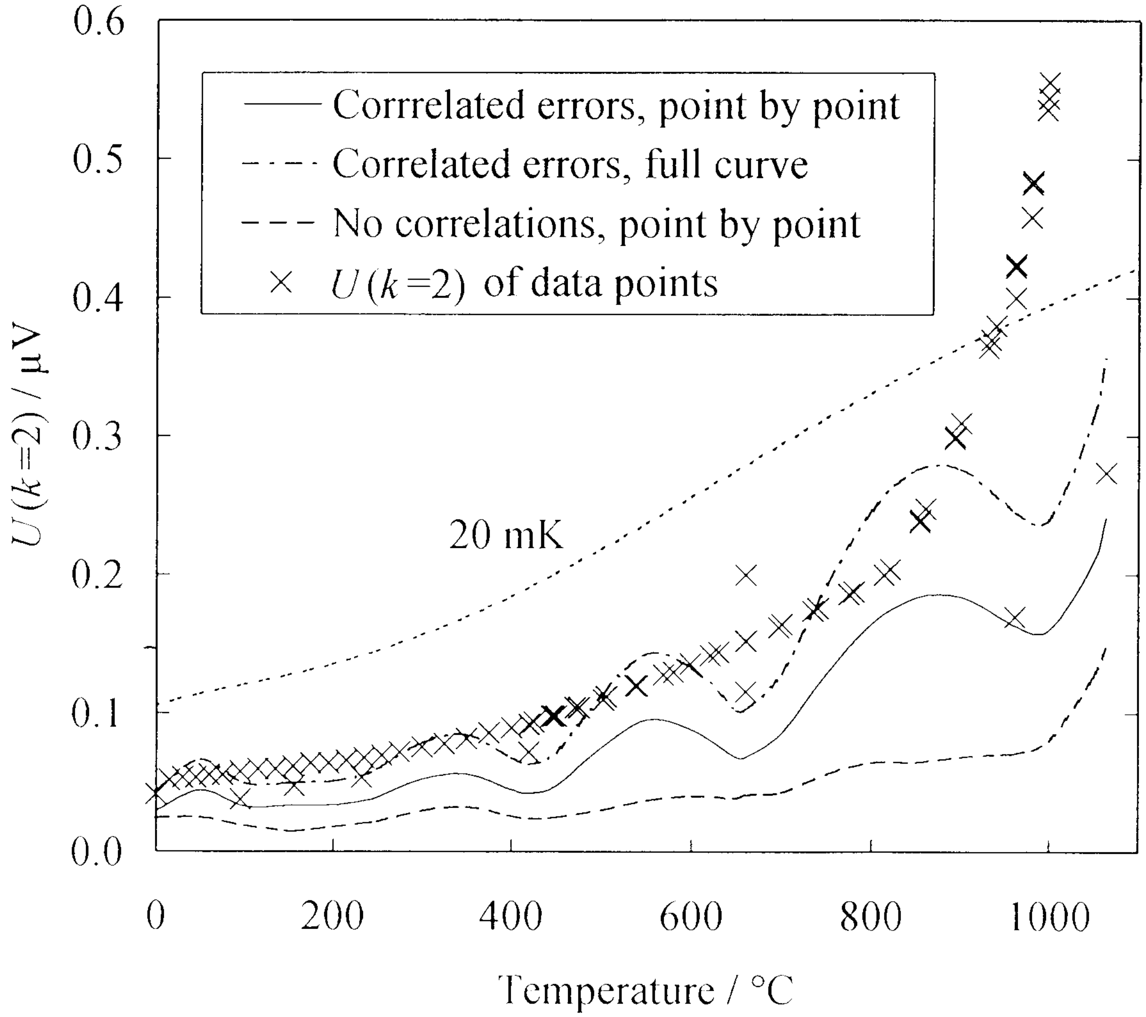
0.6
0.5
0.4
0.3
0.2
0.1
0.0
U (k=2) / µV
Corrrelated errors, point by point
Correlated errors, full curve
No correlations, point by point
U (k=2) of data points
20 mK
0
200
400
600
800
1000
Temperature / °C

Fig. 9

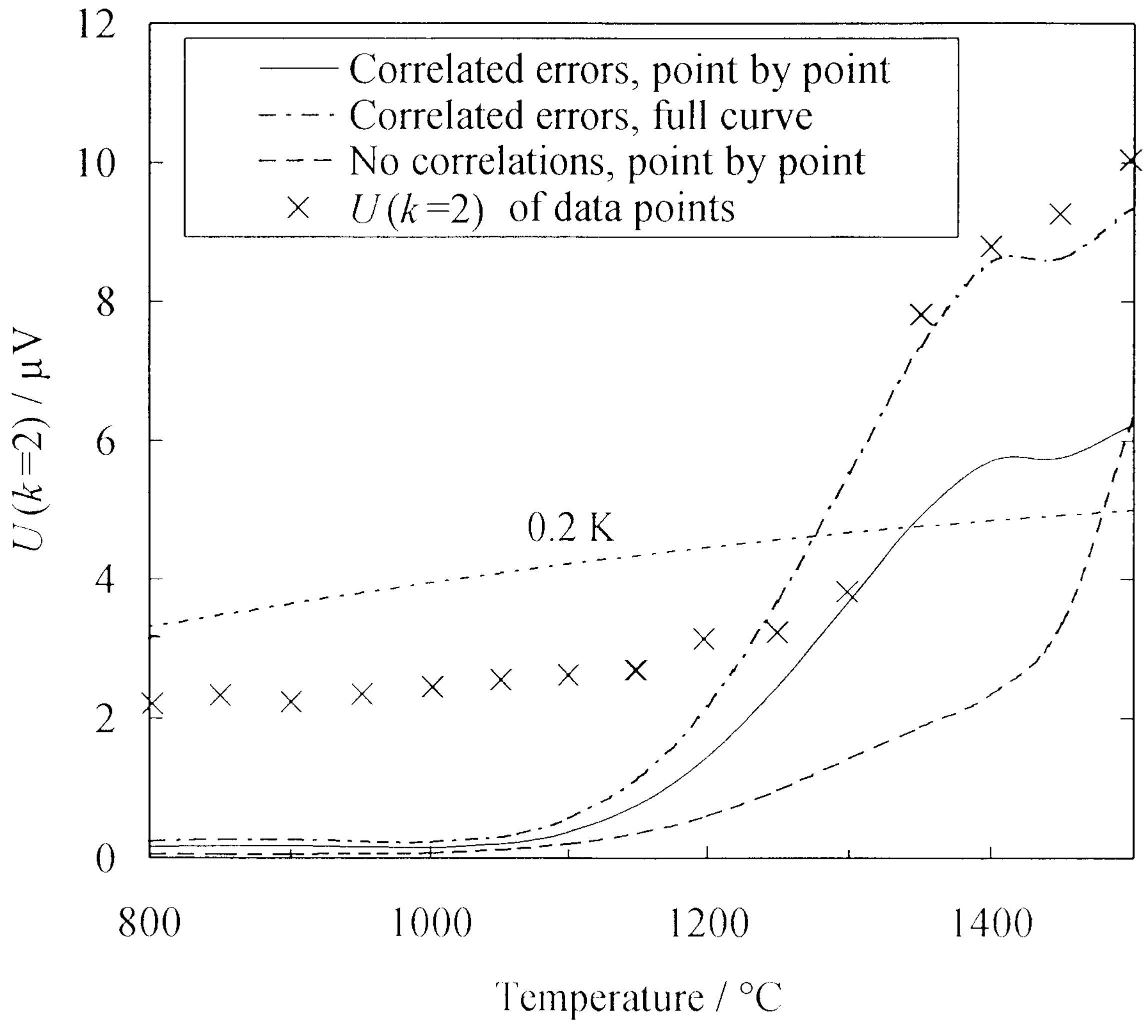

12
10
8
6
4
2
0
800
1000
1200
1400
Temperature / °C
U (k=2) / μV
Correlated errors, point by point
Correlated errors, full curve
No correlations, point by point
U (k=2) of data points
0.2 K

Fig. 10

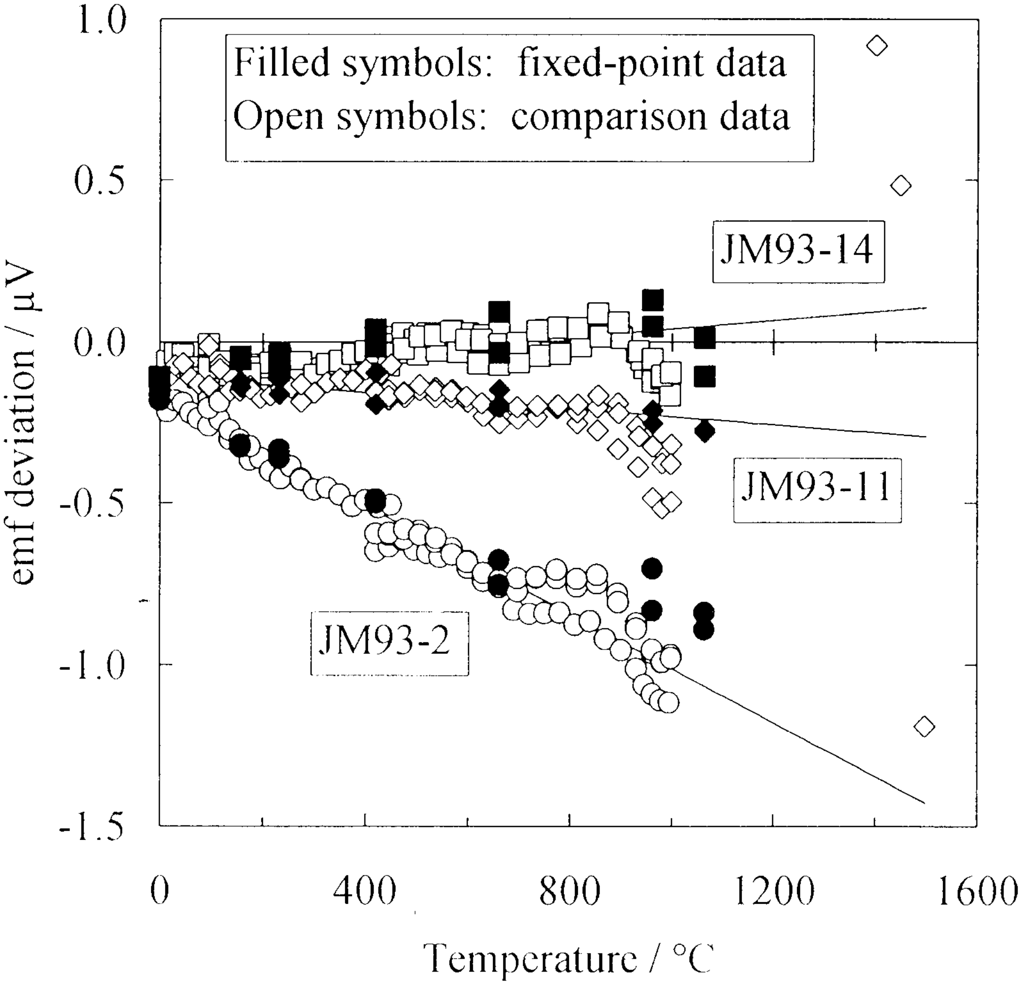

Filled symbols: fixed-point data
Open symbols: comparison data
JM93-14
JM93-11
JM93-2
emf deviation / μV
Temperature / °C
1.0
0.5
0.0
-0.5
-1.0
-1.5
0
400
800
1200
1600

Fig. 11

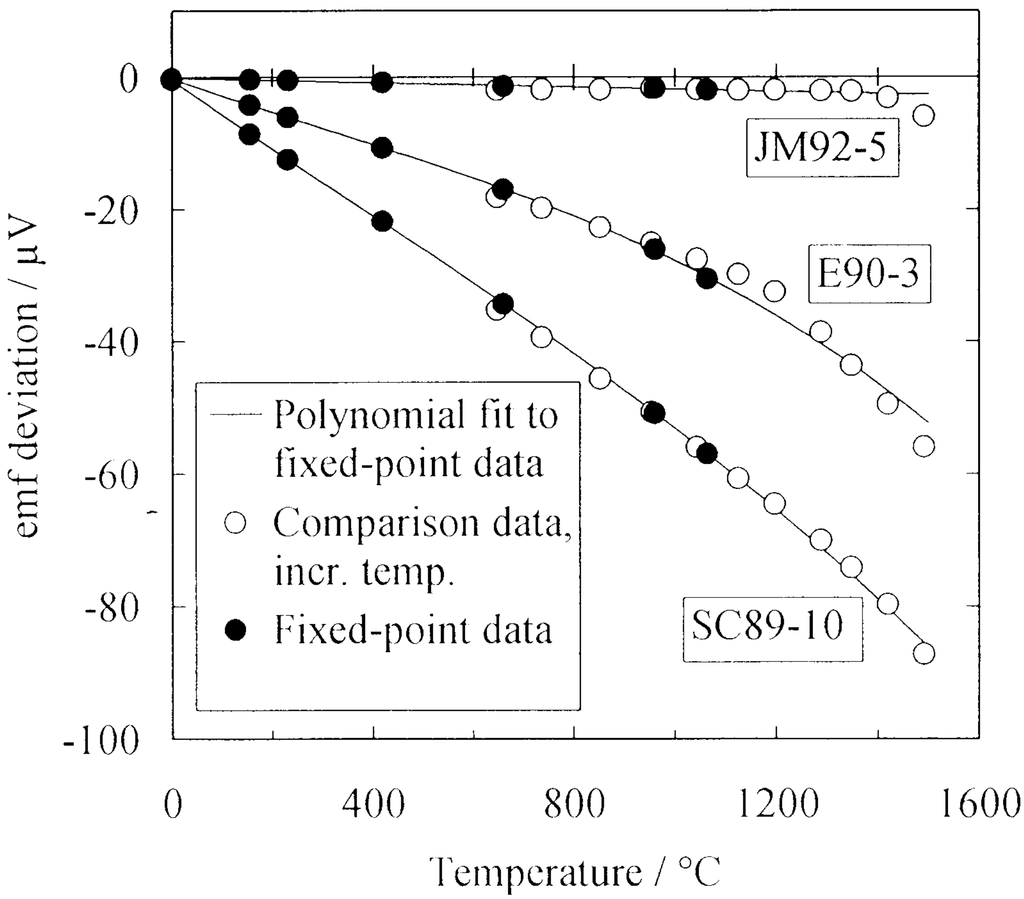

0
-20
-40
-60
-80
-100
0
400
800
1200
1600
emf deviation / µV
Temperature / °C
JM92-5
E90-3
SC89-10
Polynomial fit to fixed-point data
Comparison data, incr. temp.
Fixed-point data

Fig. 12

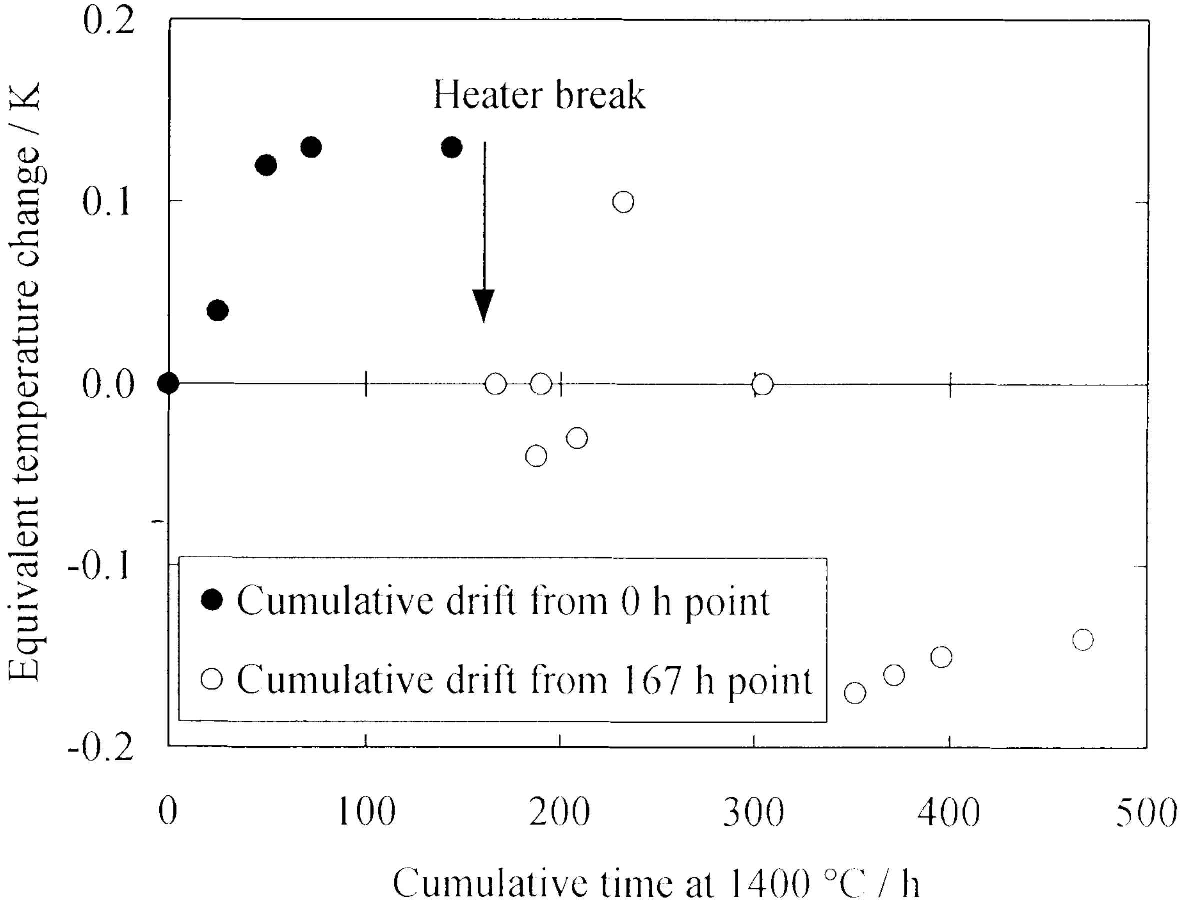
Heater break
Equivalent temperature change / K
0.2
0.1
0.0
-0.1
-0.2
0
100
200
300
400
500
Cumulative time at 1400 °C / h
Cumulative drift from 0 h point
Cumulative drift from 167 h point

Fig. 13

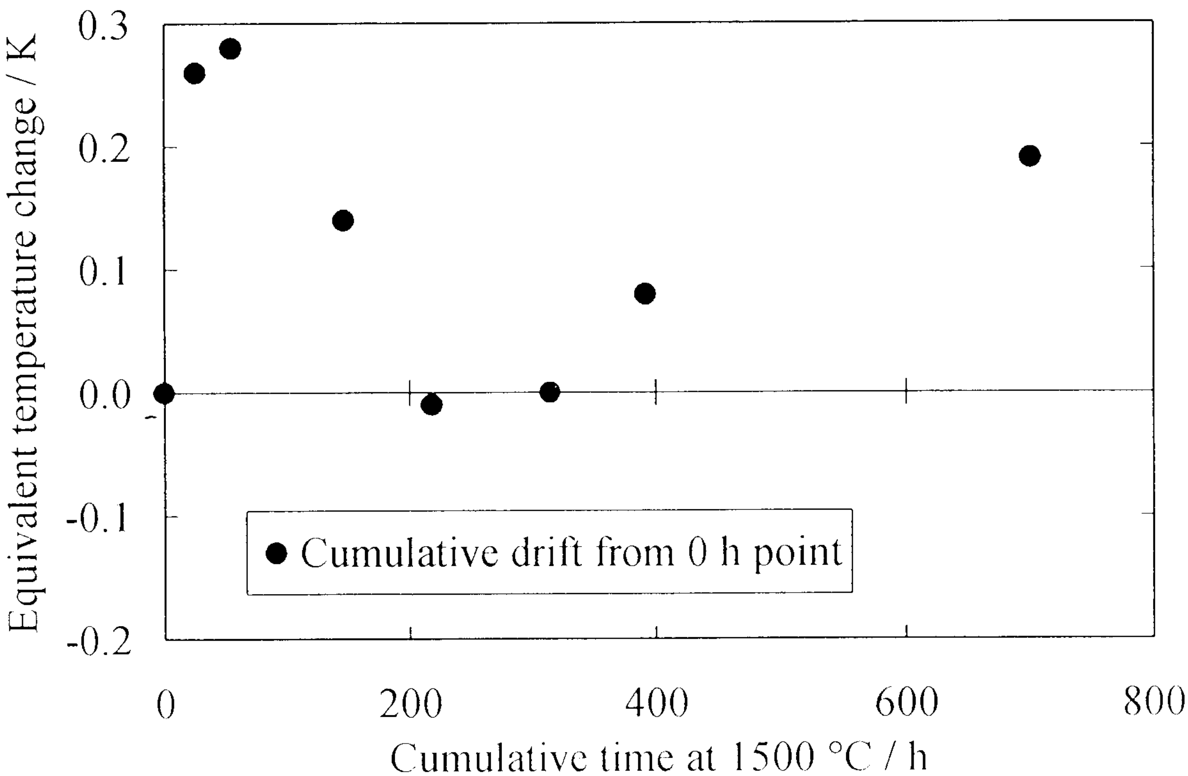
0.3
0.2
0.1
0.0
-0.1
-0.2
Equivalent temperature change / K
Cumulative drift from 0 h point
0
200
400
600
800
Cumulative time at 1500 °C / h

Fig. 14

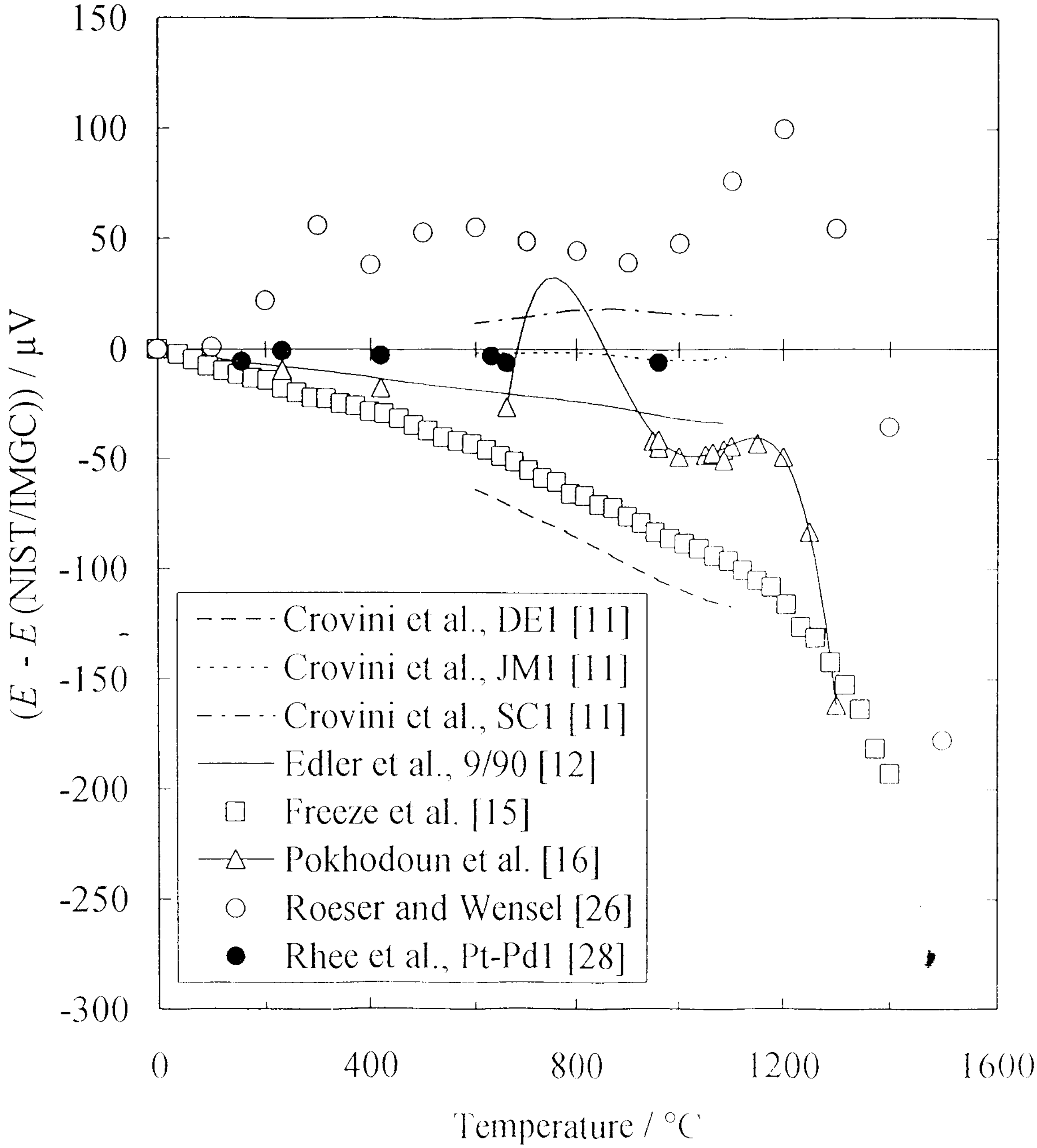

150
100
50
0
-50
-100
-150
-200
-250
-300
(E - E(NIST/IMGC)) / μV
0
400
800
1200
1600
Temperature / °C
Crovini et al., DE1 [11]
Crovini et al., JM1 [11]
Crovini et al., SC1 [11]
Edler et al., 9/90 [12]
Freeze et al. [15]
Pokhodoun et al. [16]
Roeser and Wensel [26]
Rhee et al., Pt-Pd1 [28]

Fig. 15